The role of the Arabidopsis AHL15/REJUVENATOR gene in developmental phase transitions

Karami, O.; Karami O.

Chapter 3

A molecular switch for juvenility and polycarpy in flowering plants

Omid Karami[1], Majid Khan[1], Arezoo Rahimi[1], Patrick Mak[2,3], Monique Compier[2,4] and Remko Offringa[1]

[1]Plant Developmental Genetics, Institute of Biology Leiden, Leiden University, Sylviusweg 72, 2333 BE Leiden, Netherlands
[2]Add2X Biosciences BV, Sylviusweg 72, 2333 CB Leiden, Netherlands
[3] Current address: Sanquin Plasma Products bv, Dept. Product Development, Plesmanlaan 125, 1066 CX Amsterdam, The Netherlands
[4] Current address: Rijk Zwaan, Burgemeester Crezeelaan 40, 2678 KX De Lier, Netherlands

Abstract

In flowering plants, Ageing is defined by a series of developmental phase transitions that start with vegetative growth, followed by flowering and culminating in seed production. Tissue senescence and plant death follow seed production in monocarpic plants while polycarpic plants prolong their life span by maintaining a number of vegetative axillary meristems, thereby allowing subsequent cycles of vegetative and reproductive development. Here we show that the AT-HOOK MOTIF CONTAINING NUCLEAR LOCALIZED protein AHL15/REJUVENATOR (RJV) is a suppressor of developmental phase transitions. Loss-of-function of *RJV* in *Arabidopsis* resulted in precocious appearance of adult vegetative traits and early flowering, whereas *RJV* overexpression prolonged the juvenile phase and delayed flowering in *Arabidopsis* and tobacco. We also show that RJV is a suppressor of axillary meristem maturation, with effects on plant shoot architecture and longevity. Expression of a dominant-negative *RJV-GUS* gene fusion accelerated axillary meristem maturation, whereas constitutive expression of *RJV* kept juvenile traits on axillary meristems during flowering and converted monocarpic *Arabidopsis* and tobacco plants into polycarpic plants with enhanced seed and biomass production. Our results show that *RJV* acts downstream of Ageing (*miR156*, *SPL*) and flowering (*SOC1*, *FUL*) genes as a molecular switch between monocarpic and polycarpic life history strategy, and can be used as a breeding tool to promote sustainable plant production by converting annual crops into perennial plants.

Keywords: developmental phase changes, *AHL* genes, *REJUVENATOR* gene, monocarpic, polycarpic, *Arabidopsis*, tobacco

Introduction

Plant development progresses through a fixed order of distinct phases, starting with embryogenesis and followed successively by the juvenile vegetative, adult vegetative, reproductive and gametophytic phases. During the juvenile vegetative phase the plant is usually not competent to flower. Flowering requires the transition from juvenile to adult vegetative development, which is referred to as the vegetative phase change, and is characterized by specific changes in leaf morphology (Wu and Poethig, 2006; Wu et al., 2009; Usami et al., 2009). The transition from the juvenile to the adult phase involves/requires considerable genetically pre-determined molecular and physiological changes that are also environmentally regulated (Jarillo et al., 2009; Kaufmann et al., 2010). Although all flowering plants go through the same developmental phases, there are major differences in the life span of individual plant species, which can vary from a few weeks up to several thousand years. Many flowering plant species are monocarpic: they produce seed but are unable to grow further as all their vegetative meristems are converted to reproductive meristems. Monocarpic plants are generally annual or biannual, i.e. they live one or two growing seasons, respectively. By contrast, many other flowering plant species are polycarpic: polycarpic plants generally live for more than two growing seasons (perennial), and do so by maintaining underground root stocks or axillary meristems in the vegetative state, allowing them to produce new shoots after seed set and during the next growing season (Munné-Bosch, 2008; Amasino, 2009).

The genetic basis for the monocarpic and polycarpic growth habits has been investigated in a number of cruciferous plants (Wang et al., 2009b; Zhou et al., 2013a). *Arabis alpine* and *Cardamine flexuosa* show temperature-dependent polycarpy that is regulated by the temperature sensitive repression of orthologs of the *Arabidopsis thaliana* MADS box gene *FLOWERING LOCUS C* (*FLC*), respectively *PEP1* and *CfFLC* (Wang et al., 2009b; Zhou et al., 2013a). Under higher ambient temperatures *PEP1* and *CfFLC* block the conversion of vegetative meristems into floral meristems to maintain vegetative development, but under low temperatures, during winter, cold-induced chromatin modifications repress *PEP1* and *CfFLC* expression, promoting conversion of vegetative meristems to floral mersitems and subsequent flowering in spring (Wang et al., 2009b; Zhou et al., 2013a). Despite these studies, the molecular basis for the difference between the mono- and polycarpic growth habit is still largely unknown.

Here we identify a role for the *Arabidopsis AT-HOOK MOTIF COINTAINING NUCLEAR LOCALIZED 15/REJUVENATOR* (*AHL15/RJV*) gene in the control of plant growth habit. Nuclear proteins containing one or more AT-hook motifs have been identified in all eukaryotes, where they contribute to a diverse array of crucial cellular processes (Reeves, 2010). The AT-hook motif binds to the minor groove of AT-rich DNA, and in animal cells these proteins have been found to induce changes in chromatin structure(Aravind and Landsman, 1998; Reeves, 2010). Besides the AT-hook motif, the plant-specific AHL proteins have a PPC domain that contributes to the physical interaction of AHL proteins with other nuclear proteins, such as transcription factors (Zhao et al., 2013). Other AHL proteins have been shown to be implicated in several aspects of plant growth and development in *Arabidopsis*, including hypocotyl growth (Street et al., 2008; Xiao et al., 2009; Zhao et al.,

2013), vascular tissue differentiation (Zhou et al., 2013b), flower development (Ng et al., 2009), and flowering time (Street et al., 2008; Xiao et al., 2009; Xu et al., 2013; Yun et al., 2012).

Our analyses in *Arabidopsis* and tobacco (*Nicotiana tabacum*) show that *AHL15/RJV* and its paralogs act as general suppressors of developmental phase changes. In the monocarpic plant species *Arabidopsis*, reduced A*HL15/RJV* expression coincided with a faster progression from the vegetative to the reproductive phase, during which all vegetative meristems were converted to reproductive meristems. By contrast, A*HL15/RJV* overexpression delayed the vegetative to reproductive phase change in both *Arabidopsis* and tobacco, causing some axillary meristems to be maintained in the vegetative phase, thereby allowing polycarpic development in these monocarpic annuals.

Results

Arabidopsis AHL15 and its close homologs delay the vegetative phase change and flowering

The *Arabidopsis AHL15* gene was identified in an unrelated yeast one-hybrid screen. Database analysis showed that it belonged to a large gene family of AT-hook motif nuclear proteins in *Arabidopsis*, where it grouped together with proteins containing a single AT-hook motif, among which the close paralogs *AHL19* and *AHL20* (Fig. S1A). To study the wild-type function of *AHL15*, we selected *ahl15* and *ahl19* single loss-of-function mutants (Fig. S1B), and generated a knock down for *AHL20* using an artificial microRNA (*amiRAHL20*), since a T-DNA insertion line was not available for this gene. In line with the previously reported functional redundancy between *AHL* genes (Street et al., 2008; Xiao et al., 2009; Zhao et al., 2013), *ahl15* and *ahl19* loss-of-function mutants (Fig. S1B) flowered at the same time as wild-type plants, as measured by the number of leaves at flowering (Table 1); however, an *ahl15 ahl19 amiRAHL20* triple mutant, and *ahl15/+* heterozygous mutant plants expressing a dominant negative *AHL15::AHL15-GUS* fusion (*ahl15/+ AHL15::AHL15-GUS*) showed a significant reduction in flowering time (Table 1 and Fig. S1C,D). All generated *pAHL15::AHL15-tagRFP* plant lines (n=20) showed a wild-type phenotype, but the majority of the *AHL15::AHL15-GUS* lines (n=25) flowered and senesced early (Fig. S1D). This phenotype was strongly enhanced when the *AHL15::AHL15-GUS* locus of 3 lines was combined with the heterozygous *ahl15* loss-of-function allele. In addition, approximately 25% of the seeds produced by *ahl15/+ AHL15::AHL15-GUS* plants were defective (Chapter 2, Fig. 2), and no progeny homozygous for the *ahl15* allele could be obtained, suggesting that this genetic combination is embryo lethal. In contrast, *ahl15 pAHL15::AHL15-tagRFP* plants were fertile and showed wild-type development. These results suggested that the AHL15-tagRFP fusion is functional, and that the AHL15-GUS fusion protein is inactive and has a dominant negative effect on the activity of other AHL proteins in the absence of sufficient wild-type AHL15 protein. Triple homozygous *ahl15 AHL15::AHL15-GUS AHL15::AHL15-tagRFP* plants developed normally and were fertile, corroborating that the AHL15-tagRFP protein is functional and can negate the dominant negative effect of the AHL15-GUS fusion in the *ahl15* loss-of-function mutant background.

Table 1: *AHL* genes redundantly maintain leaf juvenility and suppress flowering.

	Long days (LD)		Short days (SD)	
Genotype	# leaves w/o ab. trichom.[1]	# of rosette leaves[2]	# leaves w/o ab. trichom.[1]	# of rosette leaves[2]
Col-0	5.85 ± 0.08	16.5 ± 0.32	7.10 ± 0.10	34.02 ± 0.35
35S::AHL15-1	16.7 ± 0.42	44.35 ± 0.68 [c]	18.05 ± 0.46[c]	76.10 ± 1.19 [c]
35S::AHL15-2	14.9 ± 0.37[c]	40.55 ± 0.71 [c]	16.40 ± 0.42[c]	69.65 ± 1.18 [c]
ahl15	5.05 ± 0.05[b]	16.15 ± 0.27 [a]	5.65 ± 0.18[b]	31.40 ± 0.34[a]
ahl19	5.75 ± 0.09[a]	15.90 ± 0.33[a]	7.15 ± 0.1[a]	33.30 ± 0.36[a]
ahl15 ahl19	5.15 ± 0.08[b]	15.90 ± 0.19[a]	5.6 ± 0.21[b]	31.05 ± 0.38[a]
ahl15 ahl19 35S:amiRAHL20-1	4.90 ± 0.10[b]	13.80 ± 0.23[c]	5.10 ± 0.14[c]	25.85 ± 0.31[c]
ahl15 ahl19 35S:amiRAHL20-2	5.25 ± 0.14[b]	12.00 ± 0.16[c]	5. 30 ± 0.16[c]	22.04 ± 0.38[c]
AHL15::AHL15-GUS-1	3.90 ± 0.06[c]	10.40 ±0.24 [c]	4.25 ± 0.09 [c]	25.85 ± 0.33[c]
AHL15::AHL15-GUS-2	4.00 ± 0.06[c]	10.75 ± 0.23[c]	4.35 ± 0.13[c]	26.75 ± 0.42[c]
ahl15/+ AHL15::AHL15-GUS	3.95 ± 0.11[c]	9.20 ± 0.34[c]	4.10 ± 0.12 [c]	17.87 ± 0.46 [c]

[a] Not significantly different from wild type (Student's *t*-test, $p > 0.05$).
[b] Significantly different from wild type (Student's *t*-test, $p < 0.05$).
[c] Significantly different from wild type (Student's *t*-test, $p < 0.01$).
[1] Number of rosette leaves without abaxial trichomes.
[2] Total number of rosette leaves upon bolting. Shown is the mean ± SEM. n= 20 for all genotypes.

In *Arabidopsis*, leaf heteroblasty provides a clear indicator of the vegetative phase change. Juvenile leaves have smooth margins, are rounder (length/width ratio ca. 1) and lack abaxial trichomes, whereas adult leaves have serrated margins, are more elongated (length/width ratio ca. 1.7) and have abaxial trichomes (Telfer et al., 1997). The *ahl15* single and *ahl15 ahl19 amiRAHL20* triple loss-of-function mutants showed precocious development of adult traits, including elongated and serrated leaves (Fig. 1A,B). In wild-type *Arabidopsis*, only inflorescence meristems produced cauline leaves, whereas *ahl15 ahl19 amiRAHL20* triple mutant plants already formed cauline-like leaves during the vegetative phase (Fig. 1B, e.g. leaf number 10). Similar to *ahl15 ahl19 amiRAHL20* mutant plants, *AHL15::AHL15-GUS* rosette leaves developed a more elongated leaf blade (Fig. 1A,B), and under short day (SD) conditions abaxial trichome production was observed about three plastochrons (time between successive leaf initiation events) earlier than in wild-type plants (Table 1, under SD, in column number of leaves without abaxial trichomes). *ahl15/+ AHL15::AHL15-GUS* plants produced rosette leaves with the most strongly elongated leaf blade (Fig. 1A, B). Expression of *AHL15*, *AHL19*, and *AHL20* and of a more distantly related family member *AHL29* was negatively correlated with shoot age: expression of all four genes declined during the juvenile to adult transition (week three), when shoots and leaves started to show mature traits (Fig. 1C,D).

The above results indicate that besides their role in prolonging flowering time, *AHL* genes also function during early plant development to repress the vegetative phase change and maintain juvenile traits. Previous studies have shown that the competence to enter the reproductive phase in *Arabidopsis* is tightly associated with the vegetative phase change

(Weigel, 1995; Wu and Poethig, 2006), thus *AHL* genes might delay flowering through the maintenance of juvenile potential.

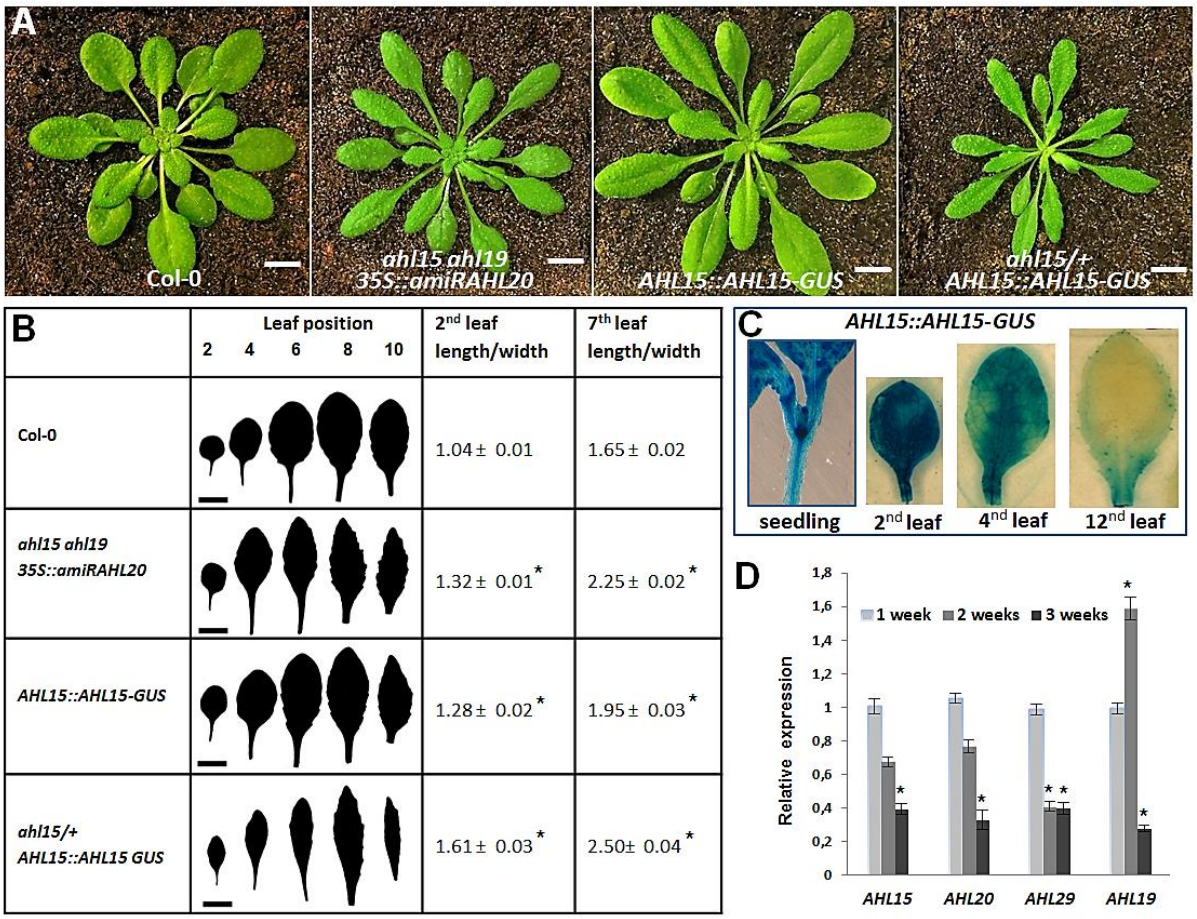

Figure 1 Arabidopsis AHL15 and close paralogs redundantly prolong leaf juvenility during vegetative development. (A) The rosette phenotype of 5-week-old wild-type (Col), *ahl15 ahl19 35S::amiRAHL20*, *AHL15::AHL15-GUS* and *ahl15/+ AHL15::AHL15-GUS* plants grown in short day (SD) conditions. (B) Overview and quantification of rosette leaf shape of wild-type, *ahl15 ahl19 35S::amiRAHL20*, *AHL15::AHL15-GUS* and *ahl15/+ AHL15::AHL15-GUS* plants grown under long day (LD) conditions. Asterisks indicate significant difference from wild-type (Student's *t*-test, $p < 0.01$) and error bars indicate standard error of the mean (n =20). (C) *AHL15::AHL15-GUS* expression in a six-day-old seedling and in juvenile and adult leaves of *AHL15::AHL15-GUS* plants under LD conditions. Leaves were harvested from one-month-old plants. (D) Quantitative RT-PCR analysis of *AHL15*, *AHL20*, *AHL29*, and *AHL19* expression in the shoot apices of one-, two-, or three-week-old seedlings grown under short day (SD) conditions. Asterisks indicate a significant difference in expression levels in one-week-old seedlings (Student's *t*-test, $p < 0.01$) and error bars indicate standard error of the mean of three biological replicates, each with three technical replicates. *β-TUBULIN-6* (At5g12250) was used as the reference gene. Size bars indicate 2 and 1 cm in A and B, respectively.

AHL15 and its paralogs promote vegetative activity of axillary meristems

The bottom nodes of wild-type *Arabidopsis* inflorescences contain an axillary meristem that produces a single cauline leaf and a lateral inflorescence. The first cauline leaves produced on wild-type primary inflorescences are phenotypically similar to rosette leaves (Fig. 2A), whereas the first cauline leaves on *ahl15/+ AHL15::AHL15-GUS* inflorescences were phenotypically more similar to the cauline leaves produced later on wild-type inflorescences (Fig. 2B). The early maturity of *ahl15/+ AHL15::AHL15-GUS* plants led to reduced cauline

leaf formation compared to wild-type plants (Fig. 2H). *AHL15::AHL15-GUS* and *ahl15/+ AHL15::AHL15-GUS* plants also senescenced earlier than wild-type plants (Fig. S2). Under SD conditions, in wild-type plants the most-basal meristems and some aerial axillary meristems continued producing rosette leaves during flowering, indicating that they were still in the vegetative phase (Fig. 3A,C). By contrast, the *ahl15/+ AHL15::AHL15-GUS* axillary meristems lost all vegetative activity after flowering under SD conditions (Fig. 3B,D). To examine whether *AHL15* expression contributed to the photoperiod-dependent fate of axillary meristems, we compered the *AHL15* expression at inflorescence nodes and axils of aerial leaves in plants grown under long day (LD) and SD conditions. GUS staining of *AHL15::AHL15-GUS* plants showed increased *AHL15* expression under SD compared to LD conditions (Fig. 3E). These data show that the *AHL15* gene acts in a photoperiod-dependent manner to promote vegetative development, and further support a role for *AHL15* and its paralogs in maintaining juvenile traits.

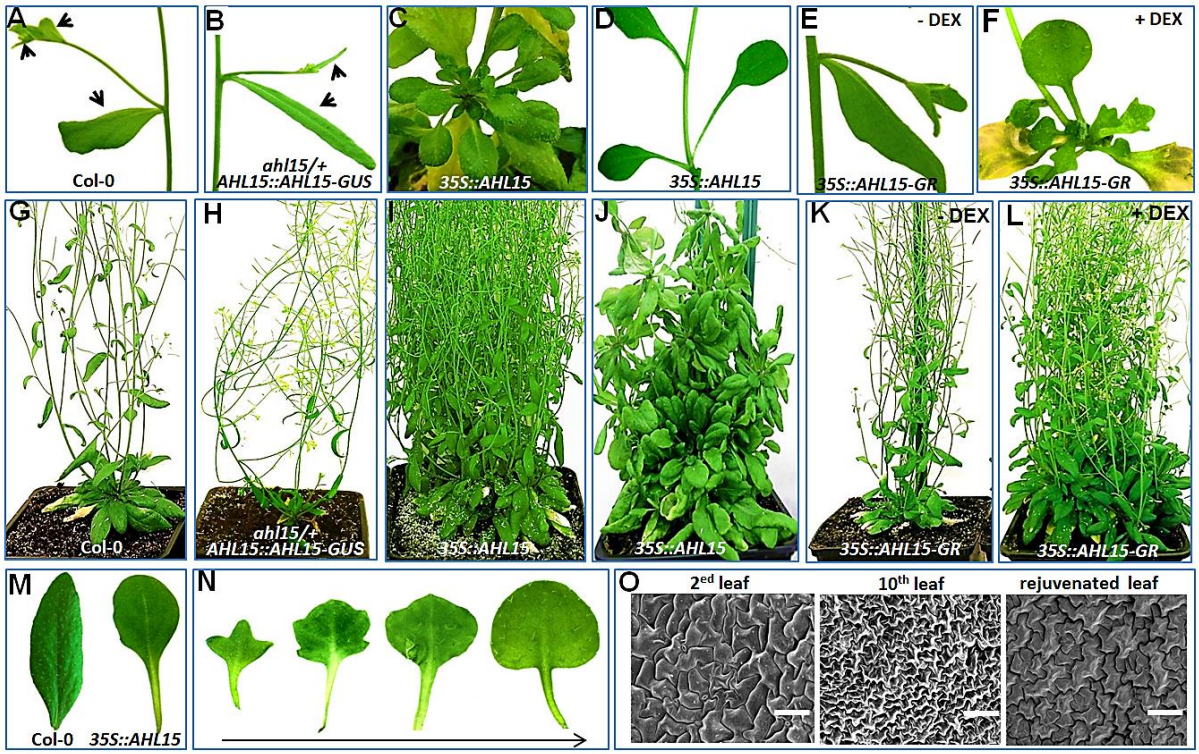

Figure 2 Ectopic *AHL15* expression in *Arabidopsis* rejuvenates axillary meristems. (A) A lateral inflorescence with fertilized flower and cauline leaves (arrow heads) formed on the first inflorescence node of a thirty five-day-old wild-type *Arabidopsis*. (B) A lateral inflorescence with fertilized flower and cauline leaf (arrow heads) formed on the first aerial node of a thirty-day-old *ahl15/+ AHL15::AHL15-GUS* plant. (C) An aerial rosette with juvenile leaves formed on the first inflorescence node of a three-month-old *35S::AHL15* plant. (D The juvenile-like cauline leaves produced on a lateral inflorescence of a 4-month-old *35S::AHL15* plant. (E) A lateral inflorescence and bract on the first inflorescence node of an untreated thirty five-day-old *35S::AHL15-GR* plant. (F) An aerial rosette with juvenile leaves developing from the first inflorescence node of a two- month-old *35S::AHL15-GR* plant two weeks after dexamethasone (DEX) application. (G-L) Mature shoot phenotypes of a flowering wild-type plant (G), a *ahl15/+ AHL15::AHL15-GUS* plant (H), a *35S::AHL15* plant (I), a *35S::AHL15* plant (J), an untreated *35S::AHL15-GR* plant (K), and a *35S::AHL15-GR* plant sprayed with DEX (L). Plants in A-I and K, L were grown under long day conditions, the plant in J under short day conditions. (M) Wild-type (Col-0) and the juvenile-like *35S::AHL15* cauline leaf. (N) Sequential leaves of an aerial rosette produced from an axillary meristem of a *35S::AHL15-GR* plant after DEX application. Leaves were harvested from two-month-old plants. (O) Scanning electron micrographs of *35S::AHL15-GR* epidermal leaf cells from respectively the 2nd rosette leaf, the 10th rosette leaf and a juvenile-like leaf produced from an axillary meristem on a two-month-old plant treated with DEX. Size bar indicates 50 μm.

Ectopic expression of *AHL15/REJUVENATOR* reverses developmental transitions in *Arabidopsis*

To substantiate the role of *AHL15* in repressing the vegetative phase change and flowering, we ectopically expressed the gene under control of the strong *CaMV 35S* promoter. *35S::AHL15* seedlings initially developed very slowly, but plants recovered three to four weeks after germination and produced rosettes and inflorescences. We noticed, however, that from the point of growth recovery these overexpression plants showed a significant delay in flowering. They produced more than twice the number of rosette leaves before bolting compared to wild-type plants, both under LD and SD conditions (Table 1 and Fig. S1D). The delay in flowering in *AHL15* overexpressing plants correlated with a significant increase in the production of juvenile leaves lacking abaxial trichomes (Table 1). These *35S::AHL15* early juvenile leaves showed a stronger reduction in adaxial trichome number and were significantly smaller than wild-type juvenile leaves up to the seventh leaf stage.

In contrast to the cauline leaf and lateral inflorescence formed at bottom nodes of wild-type *Arabidopsis* inflorescences (Fig 2A,G,M), the axillary meristems at the most basal and some aerial nodes of *35S::AHL15* inflorescences first produced a cauline leaf followed by several juvenile-like-leaves (Fig. 2C,D), eventually leading to the formation of aerial rosettes (Fig. 2I,J). Since the juvenile-like leaves and aerial rosettes (Fig. 2M) were produced after a wild-type looking cauline leaf (Fig. 2C), this suggested that ectopic *AHL15* expression induced rejuvenation of these meristems. To test the capacity of *AHL15* to rejuvenate plant tissues, we generated lines that express a fusion protein between AHL15 and the rat glucocorticoid receptor (GR) under control of the *CaMV 35S* promoter (*35S::AHL15-GR*), rendering the nuclear import and thus the activity of the ectopically expressed AHL15-GR fusion inducible by the glucocorticoid hormone dexamethasone (DEX). Untreated *35S::AHL15-GR* plants showed a wild-type phenotype (Fig. 2E,K). By contrast, after spraying forty five-day-old flowering *35S::AHL15-GR* plants with DEX, most of the basal and aerial axillary meristems produced small rosette leaves, initially resembling the small first leaves of *35S::AHL15* plants, and later producing normal juvenile leaves without abaxial trichomes (Fig. 2F,N). In these juvenile aerial rosettes the vegetative phase change occurred two to three weeks after DEX treatment, resulting in the production of adult rosette leaves. A second DEX application, four weeks after the first one, again reverted many axillary meristems to vegetative meristems, resulting in abundant production of aerial rosettes (Fig. 2L), whereas non-treated inflorescences only produced a few cauline leaves (Fig. 2K).

The vegetative phase change in *Arabidopsis* is accompanied by a decrease in leaf epidermal cell size (Usami et al., 2009). To confirm rejuvenation by ectopic *AHL15* expression, we compared the cell size of early juvenile, adult and rejuvenated leaves in *35S::AHL15-GR* plants before and after DEX treatment. The epidermis cells in DEX-treated *35S::AHL15-GR* aerial rosette leaves were significantly larger than those in adult leaves and strikingly similar in size to the second juvenile leaf produced after germination (Fig. 2O).

The above data provide evidence, both through loss-of-function and ectopic expression, that the AHL15 protein represses and can even reverse two major developmental phase transitions in plant development, the transition from vegetative to reproductive development, and the transition from juvenile to adult development. AHL15 was named REJUVENATOR (RJV) because of its generic capacity to rejuvenate plant tissues.

Overexpression of the *Arabidopsis AHL* family members *AHL19*, *AHL20*, *AHL27* and *AHL29*, and two possible *AHL15* orthologs from *Brassica oleracea* and *Medicago truncatula* in *Arabidopsis* resulted in similar morphological changes as observed for *35S::AHL15* plants, i.e. a shift from mono- to polycarpic life style/growth habit through the continuous production of aerial rosettes (Fig. S3). These results corroborated the previously observed co-regulation and functional redundancy among *Arabidopsis AHL* family members (Fig. 1, Table 1, and Fig. S1 in this paper, (Street et al., 2008; Xiao et al., 2009; Zhao et al., 2013), and suggest that the rejuvenation function of *AHL15* is conserved in dicotyledonous plant species.

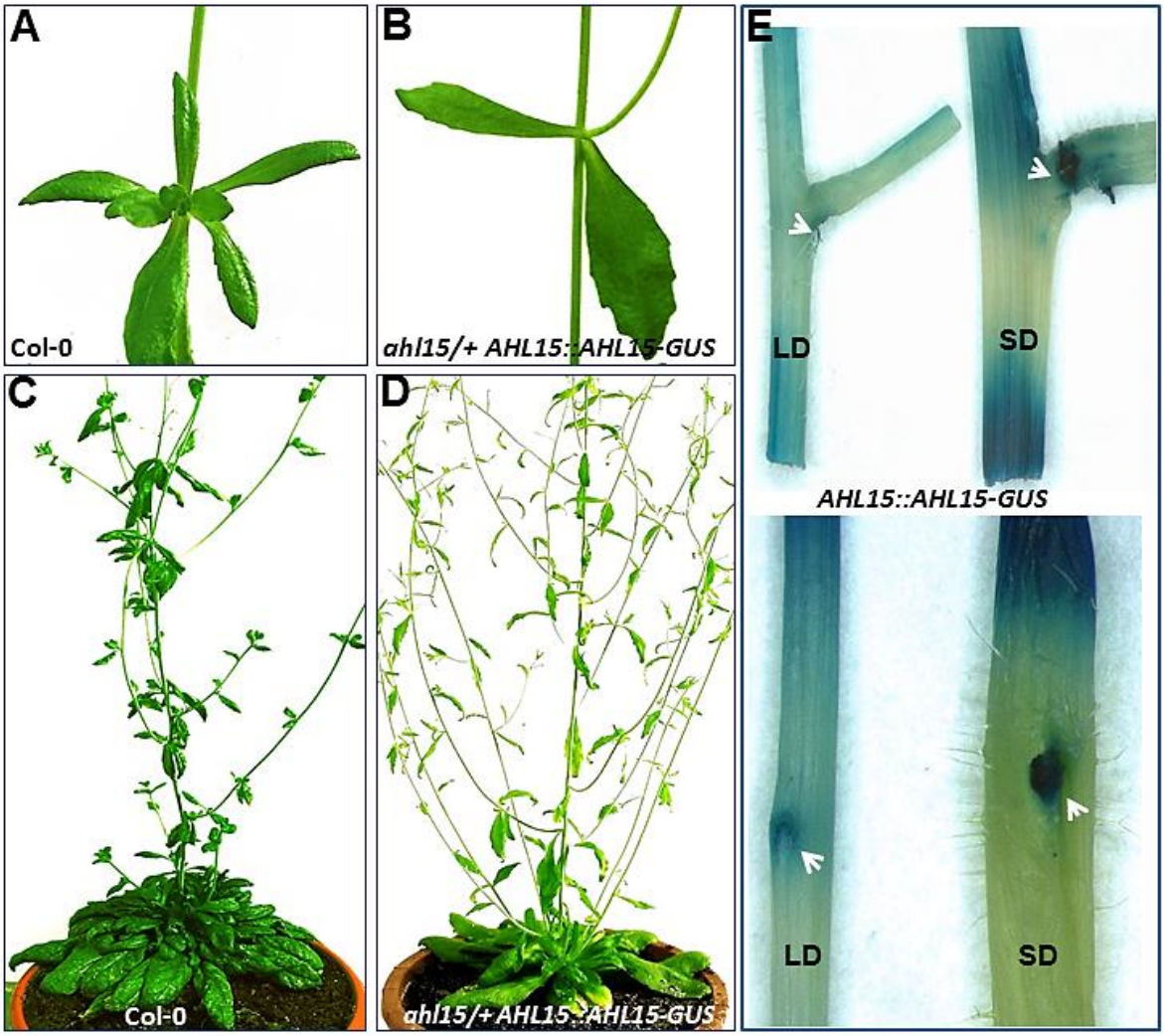

Figure 3 ***AHL*** **genes are essential for SD-induced vegetative axillary meristem activity in** ***Arabidopsis*****.** (A) A lateral inflorescence with an aerial rosette formed on the first inflorescence node of a two-month-old wild-type *Arabidopsis* plant grown under SD. (B) A lateral inflorescence and cauline leaf formed on the first aerial node of a two-month-old *ahl15/+ AHL15::AHL15-GUS* plant grown under SD. (C,D) Mature shoot phenotype of wild-type (C and *ahl15/+ AHL15::AHL15-GUS* (D) plants grown under SD. (E) GUS staining showing a higher level of *AHL15-GUS* expression in the first inflorescence node (top, arrowhead) and axil of a cauline leaf (bottom, arrowhead) of SD grown plants (left) than of LD grown plants (right). Inflorescence stems were harvested three weeks after flowering time.

Ectopic *AHL15/RJV* expression converts monocarpic *Arabidopsis* into a polycarpic woody plant

Arabidopsis is a typical annual monocarpic plant with a growth cycle of approximately 3 months. Following vegetative growth, plants bolt and produce several inflorescences with cauline leaves and flowers. Depending on the number of fruits and seeds produced, the activity of the inflorescence meristems arrests, and the plant senesces(Hensel et al., 1993; Bleecker and Patterson, 1997). Several related species, such as *Arabis alpina*, are perennial polycarpic plants that flower and produce seeds multiple times[8]. In contrast to the monocarpic life style of wild-type *Arabidopsis*, *AHL15* overexpression plants continued to grow vegetatively for several months after the first cycle of flowering and seed set by producing new aerial rosettes (Fig. 4A). These aerial rosettes produced new inflorescences, resulting in enhanced shoot branching (Fig. 3D) and a significant increase in seed yield (Fig. 4B). Removal of the terminated inflorescences with ripened siliques induced the production of new aerial rosettes (Fig. 4C) that again produced inflorescences with cauline leaves and flowers (Fig. 4E). Continuous removal of the terminated inflorescences and continuous supply of fertilizer allowed plants to produce new inflorescences and new seeds following each cutting for the 9 month period that was tested. The same phenotypes were observed in DEX-treated *35S::AHL15-GR* plants. Moreover, DEX-treated *35S::AHL15-GR* plants already produced aerial vegetative growth and new inflorescences while the first batch of siliques was still ripening (Fig. 4F).

Many polycarpic (perennial) plant species are woody, and a continuous ring of xylem, indicative of secondary growth and wood formation, can already be observed in young stems (Gerttula et al., 2015). Inflorescence stems of herbaceous monocarpic species such as *Arabidopsis* show secondary xylem development, but do not form the regular xylem cylinder that precedes wood formation (Fig. 5A,B). In line with their polycarpic behaviour, *35S::AHL15* plants developed a complete xylem ring in their primary inflorescence stems as early as two weeks after the induction of flowering (Fig. 5C) and a solid wood cylinder was established in the main and lateral inflorescences of four-month-old plants (Fig. 5D). The fact that secondary growth can be observed early during inflorescence development, suggests that it is not an indirect effect of the enhanced and prolonged inflorescence development in *AHL15* overexpression plants, but rather, that ectopic *AHL15* expression directly triggers cambium activity resulting in wood development.

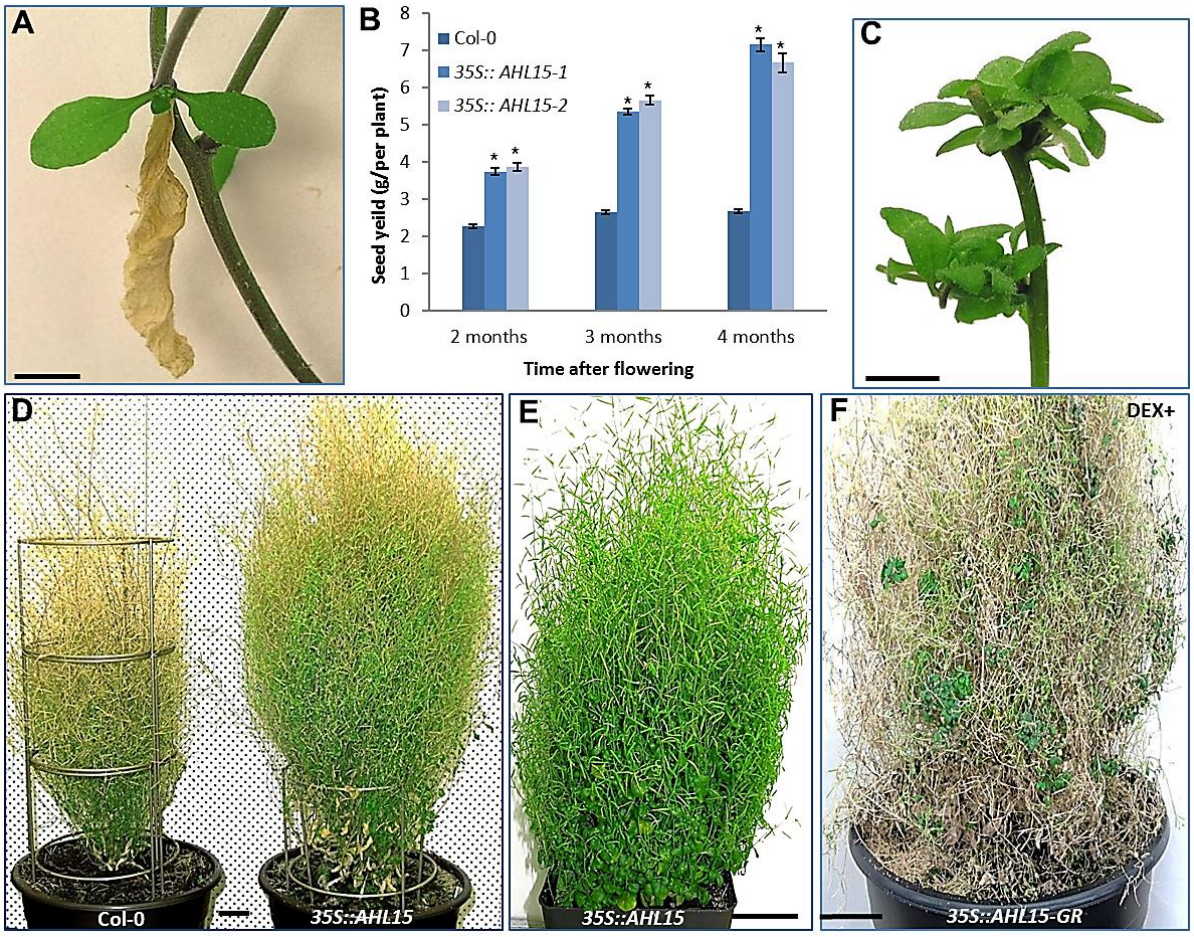

Figure 4 Ectopic *AHL15* expression converts monocarpic *Arabidopsis* into a polycarpic plant. (**A**) Development of an aerial rosette from an axillary meristem on an inflorescence of a four-month-old *35S::AHL15* plant. The senesced cauline leaf indicates that the rosette developed after seed ripening. (B) Comparison of seed yield of wild-type and *35S::AHL15* plants grown under LD for the indicated time. Asterisks indicate a significant difference from wild type (Student's *t*-test, $p < 0.01$), and error bars indicate standard error of the mean (n=6). (C) Efficient production of aerial rosettes in a 5-month-old *35S::AHL15* plant from axillary meristems just below the positions where inflorescences were cut to harvest the seeds. (D) Inflorescence branching of wild-type (left) and *35S::AHL15* (right) plants 3 months after flowering. (E) Efficient production of inflorescences and new seed set in a five-month-old *35S::AHL15* plant after the first seed harvesting. (F) Renewed vegetative growth on aerial branches of a five-month-old *35S::AHL15-GR* plant and sprayed with 20 µM DEX (no seed were harvested yet). Plants in A-F were grown under LD conditions. Size bars indicate 1 cm in A and C and 4 cm in D, E and F.

Arabidopsis AHL15/RJV induces juvenile traits and polycarpy in tobacco

We determined whether heterologous *AHL15* expression could also induce similar developmental changes in a non-related plant species. We introduced the *35S::AHL15-GR* construct into tobacco. Young DEX-treated *35S::AHL15-GR* plants formed small, round juvenile leaves, whereas untreated transgenic plants produced only three juvenile leaves before producing the typically larger and longer adult tobacco leaves (Fig. 6A). This result indicates that *AHL15* expression extends the juvenile phase in tobacco, as in *Arabidopsis*.

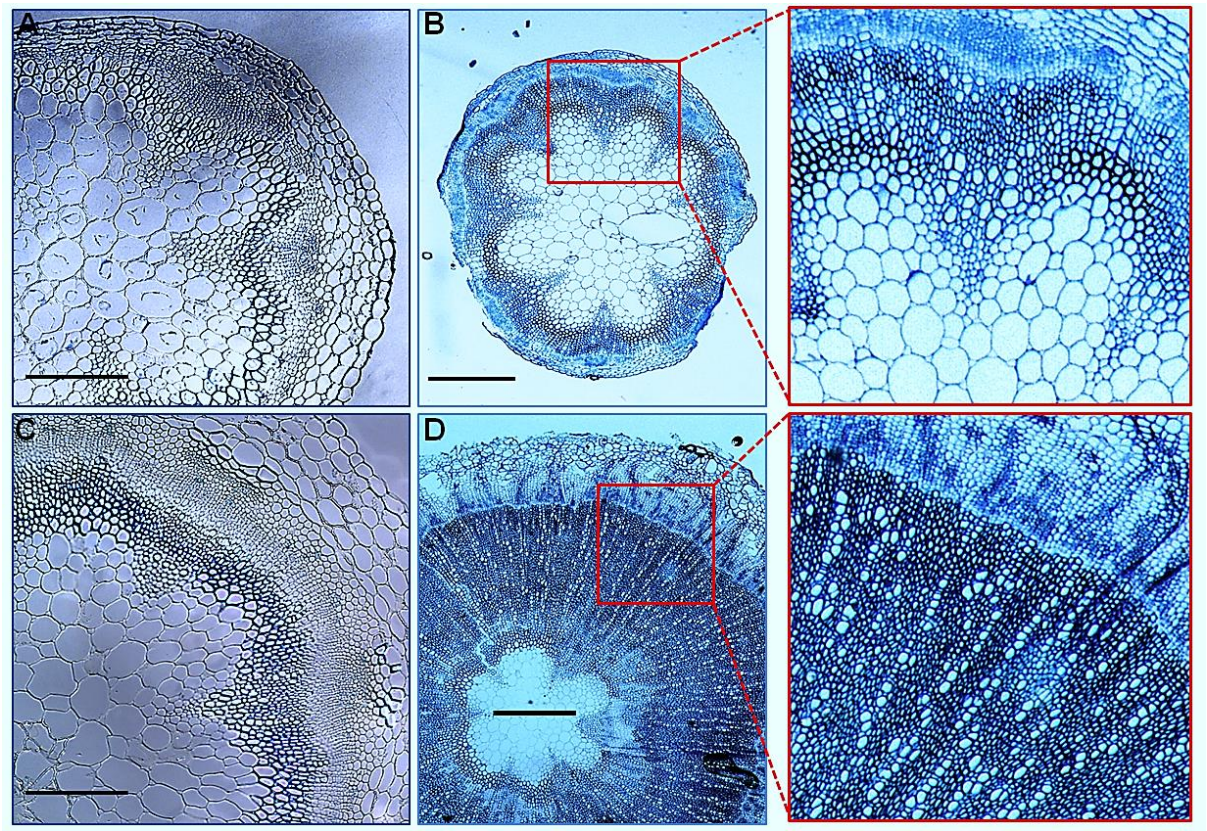

Figure 5 Secondary growth in wild-type and *35S::AHL15 Arabidopsis* inflorescence stems. (A,B) Cross-section of the main inflorescence stem of a two-week-old (A, 4-5 mm above the rosette) or two-month-old (B, 5-7 mm above the rosette) wild-type plant. (C,D) Cross-section of the main inflorescence stem of a 2-week-old (C, 4-5 mm above the rosette) or three-month-old (D, 5-7 mm above the rosette) *35S::AHL15* plant. Cross-sections were stained with toluidine blue. Size bars in a to D indicate respectively 100, 200, 150 and 500 µm.

DEX-treated *35S::AHL15-GR* tobacco plants continued to produce small juvenile leaves for six months before flowering and from axillary meristems during flowering (Fig. 6B), and showed reduced apical dominance, resulting in enhanced shoot branching and enhanced production of leaves and inflorescences (Fig. S4A). Axillary meristems in DEX-treated *35S::AHL15-GR* were also able to resume growth after the first seed set (Fig. 6D), whereas wild-type and non-treated *35S::AHL15-GR* plants arrested growth and senesced after seed set (Fig. 6C). After the second seed batch produced by the now seven month-old DEX treated *35S::AHL15-GR* plants (Fig. 6E) were harvested, the plants were treated with DEX for a third, fourth and fifth cycle, which efficiently induced vegetative growth and subsequent flowering and seed set, allowing the *35S::AHL15-GR* plants to survive for more than 2 years (Fig. S4B). The production of juvenile-like leaves on DEX sprayed axillary meristems of *35S::AHL15-GR* plants (Fig. 6F) indicated that, as in *Arabidopsis*, the polycarpic behaviour of DEX treated *35S::AHL15-GR* tobacco plants was caused by rejuvenation of axillary meristems.

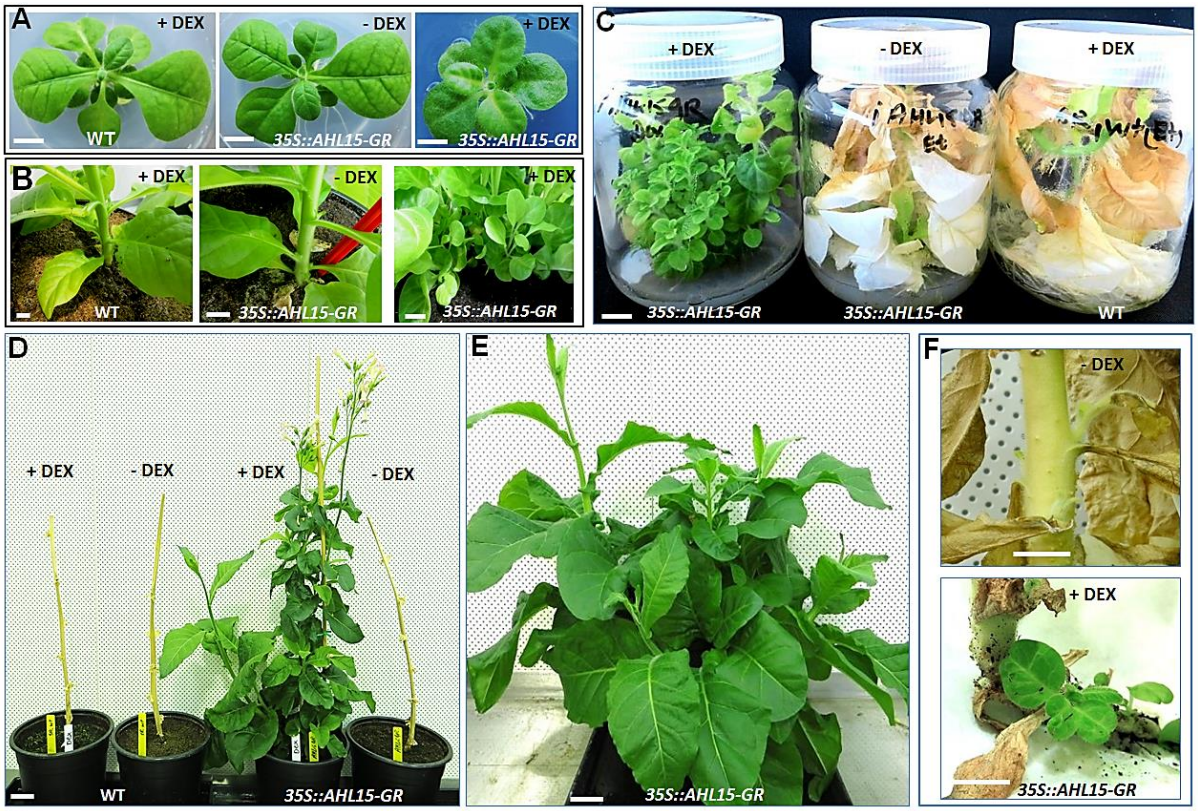

Figure 6 Heterologous *AHL15* expression rejuvenates axillary meristems and induces polycarpy in tobacco. (A) Shoot morphology of axenically grown one-month-old wild-type (left) and *35S::AHL15-GR* (middle and right) plants on media with 10 µM DEX (left and right) or without DEX (middle). (B) Differential activity (formation juvenile-like leaves) of axillary meristems in flowering 30 µM DEX-sprayed wild-type (left) or untreated *35S::AHL15-GR* (middle) plants, versus 30 µM DEX-sprayed *35S::AHL15-GR* plants (right). (C) Enhanced shoot development on axenically grown four-month-old *35S::AHL15-GR* plants (right) on media with DEX (left) versus senesced plants on medium without DEX (middle) or senesced wild-type plants on medium with10 µM DEX (right). (D) Growth response to DEX spraying in five-month-old wild-type (left) and *35S::AHL15-GR* (right) plants. (E) Efficient production of new leaves and subsequently inflorescences in a seven-month-old *35S::AHL15* plant after DEX treatment. (F) Axillary meristem activity before (upper panel) and 10 days after 30 µM DEX treatment (lower panel) in a 1 year-old *35S::AHL15-GR* plant. Size bars indicate 1cm in A, B, C and F and 5 cm in D and E.

AHL15/RJV acts downstream of Ageing (miR156, SPL) and flowering (SOC1, FUL) genes

During the *Arabidopsis* life cycle the gradual decrease in *microRNA156* (*miR156*) expression results in increased expression of the *SQUAMOSA-PROMOTER BINDING PROTEIN-LIKE (SPL) miR156* target genes. *SPL* genes in turn promote the adult developmental program at the shoot apical meristem (SAM), resulting in the transition from juvenile to adult leaf production and eventually from vegetative to reproductive development (Wang et al., 2009a; Wu et al., 2009). The effect of *miR156* and *SPL* genes on AMs, however, has not been described. We therefore investigated the relationship between *miR156/SPL*- and *AHL* in the control of AM maturation. *miR156* promoter-*GUS* fusions were expressed in the basal part of the rosette in flowering *Arabidopsis* plants (Fig. 7A), explaining the enhanced SPL9 expression in *miR156* target mimic (*35S::MIM156*) (Franco-Zorrilla et al., 2007) and *miR156*-insensitive *SPL* lines (*SPL9::rSPL9*, Fig. 7B) (Wu et al., 2009). We observed

reduced cauline leaf formation and branching in *35S::MIM156* and *SPL9::rSPL9* plants, indicating precocious maturation of AMs (Fig. S5A,B), while, reducing *SPL* expression by overexpressing *miR156* (*35S::miR156*) or by *spl9 spl15* loss-of-function led to the production of rosette leaves from the AMs during flowering (Fig. S6), and induced polycarpic behaviour (Fig. 8A and Fig. S7). These results indicated that *miR156* prevents precocious maturation of AMs by suppressing *SPL* gene expression.

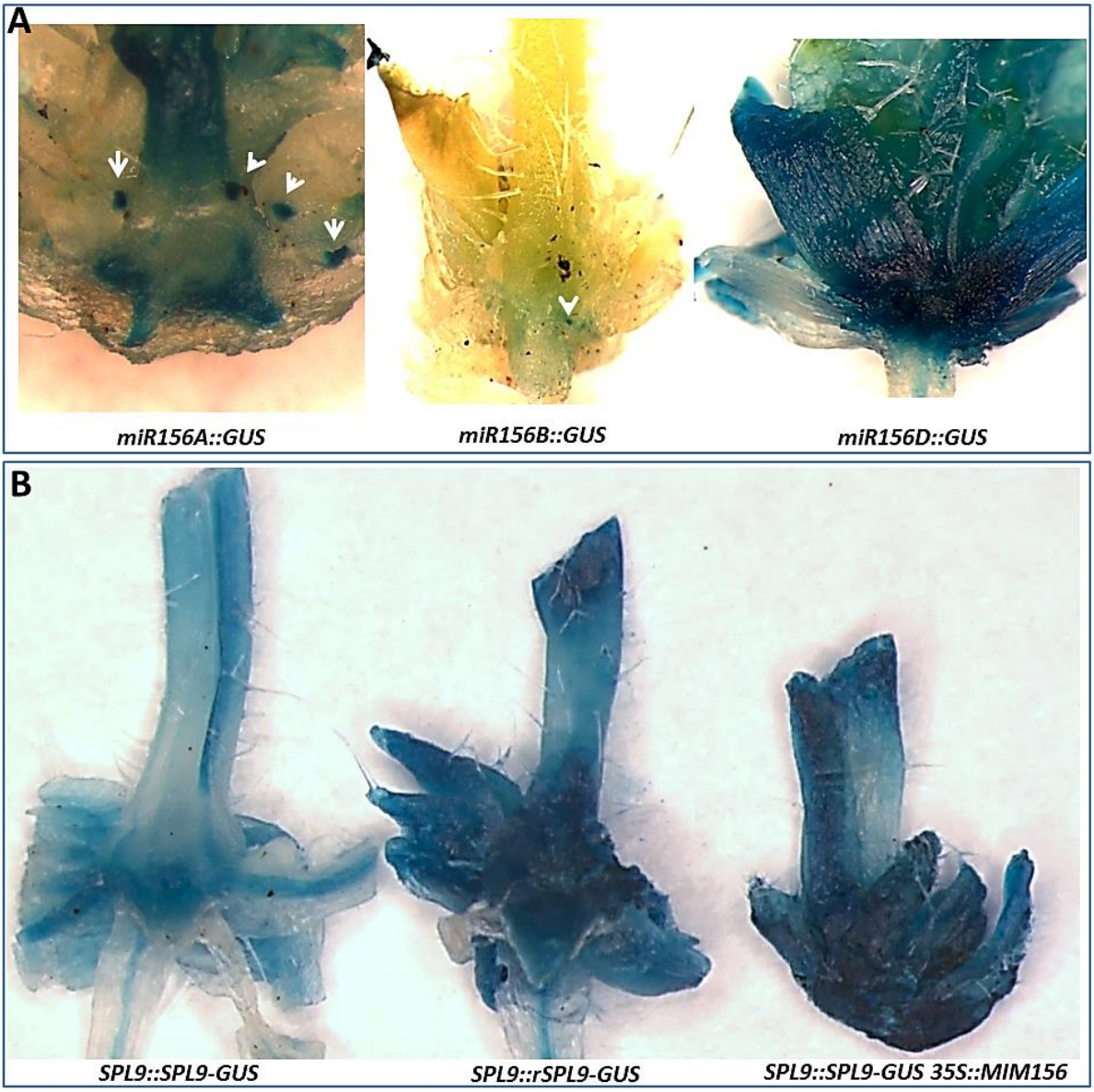

Figure 7 *miR156* reduces SPL9 expression in AMs and the rosette base of flowering *Arabidopsis* plants. (A) Expression pattern of *miR156* promoter-*GUS* gene reporters (*miR156A::GUS*, *miR156B::GUS*, *miR156D::GUS*) in AMs (arrowheads) and the rosette base of *Arabidopsis* plants 1week after flowering. (B) Expression of miR156-sensitive *SPL9::SPL9-GUS* (left) compared to the miR156-resistant SPL9::rSPL9-GUS (middle) in the rosette base of wild-type *Arabidopsis* 1week after flowering, or to *SPL9::SPL9-GUS* in *35S::MIM156* background . Plants were grown under LD.

Interestingly, *AHL15/RJV* overexpression negated the precocious maturation of AMs in *35S::MIM156* and *SPL9::rSPL9* plants (Fig. S5A,B), and dramatically enhanced the polycarpic behaviour of *35S::miR156* plants (Fig. 8A). In addition, *AHL15/RJV* function was required for the aerial rosette leaf formation and polycarpy phenotypes observed in *35S::miR156* and *spl9 spl15* plants (Fig. 8A, Fig. S6 A-D and Fig. S 7). Consistent with these results, *AHL15/RJV* and its paralog *AHL20* were strongly expressed in *35S::miR156* and *spl9 spl15* AMs (Fig. 8B,C) and showed reduced expression in *35S::MIM156* and *SPL9-rSPL9* inflorescence nodes (Fig. 8D). Based on these results, we concluded that *AHL15/RJV* and *AHL20* act downstream of the *SPL* genes. In wild-type plants *AHL* repression by SPLs promotes AM maturation, whereas under conditions where SPL activity is reduced (e.g. in *35S::miR156* or *spl9 spl15* plants) AHLs delay AM maturation, which in the case of *35S::miR156* leads to rejuvenation resulting in aerial rosette phenotypes and polycarpy.

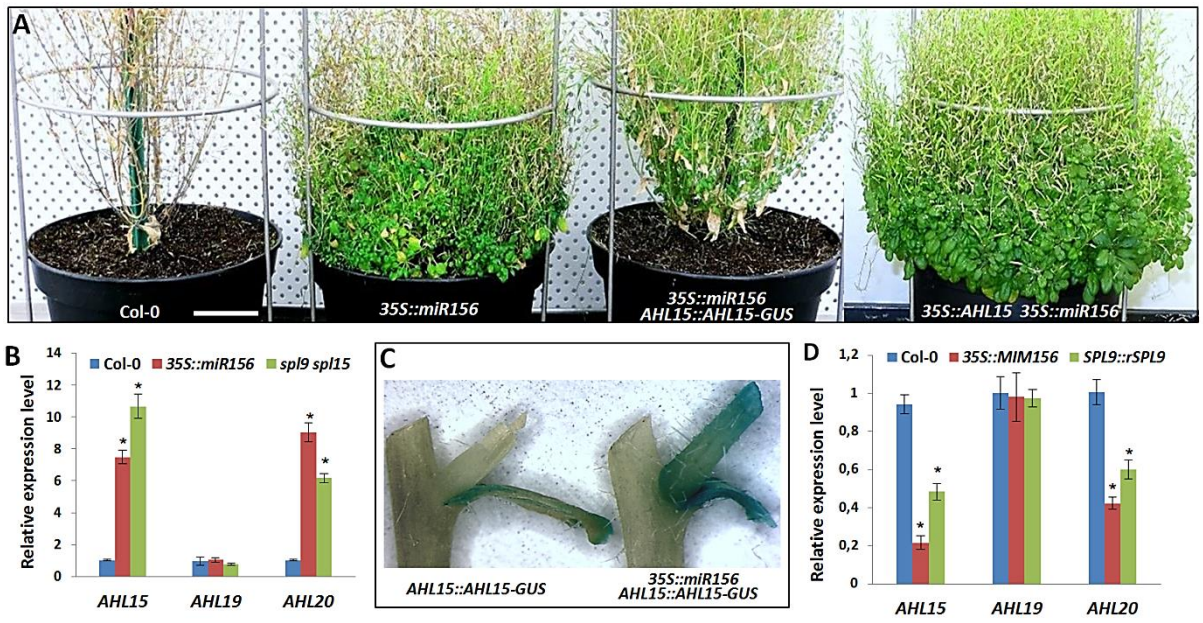

Figure 8 The miR156-regulated SPL pathway contributes to AM maturation by suppressing *AHL* genes expression. (A) Phenotype of four-month-old wild-type (Col-0), *35S::miR156*, *35S::miR156 AHL15::AHL15-GUS*, or *35S::miR156 35S::AHL15* plants, respectively. (B) Quantitative RT-PCR (qPCR) analysis of *AHL15/19/20* expression in inflorescence nodes of wild-type, *35S::mirR156* or *spl9 spl15* plants 2 weeks after flowering. (C) GUS activity showing *AHL15::AHL15-GUS* expression in an inflorescence node of six week-old wild-type and *35S::mirR156* plants. (D) qPCR analysis of *AHL15*/*19*/*20* expression in inflorescence nodes of wild type, *35S::MIM156* or *SPL9::rSPL9* plants 2 weeks after flowering. In B and D asterisks indicate a significant difference in expression level in the mutant compared to wild-type plants (Student's *t*-test, $p < 0.001$) and error bars indicate standard error of the mean of three biological replicates. Plants in A-D were grown under LD conditions. Size bars indicate 5 cm in A.

Previously, a double loss-of-function *Arabidopsis* mutant of the *SUPPRESSOR OF CONSTANS 1* (*SOC1*) and *FRUITFULL* (*FUL*) genes was found to show a perennial lifestyle (Melzer et al., 2008), with similar phenotypes as *35S::AHL15* plants. Interestingly, the *soc1 ful* double mutant in the *ahl* dominant negative loss-of-function mutant background completely lost its perennial features (Fig. 9A), suggesting that AHL function is normally repressed by SOC1 and FUL, and that *AHL* upregulation plays a key role in acquiring the

perennial lifestyle. Expression analysis using qRT-PCR (Fig. 9B) and the *AHL15::AHL15-GUS* reporter (Fig. 9C,D) showed that *AHL15/RJV* and *AHL20* were strongly upregulated in *soc1 ful* inflorescence nodes and lateral inflorescences, thereby corroborating that *AHL* genes are suppressed by SOC1 and FUL. *AHL19* transcription was unchanged in the *soc1 ful*, *35S::miR156* or *spl9 spl15* mutant lines relative to wild type (Fig. 8B and Fig. 9B), indicating that *AHL19* is not regulated by either SPL or SOC1/FUL. Previously, it was been shown that SPL proteins promote *SOC1* and *FUL* expression (Wang et al., 2009a; Yamaguchi et al., 2009) and that SOC1 binds to the *AHL15/RJV* upstream and downstream regions (Immink et al., 2012; Tao et al., 2012). Consistent with these and our findings, we postulate that SPLs promote AM maturation by upregulating *SOC1* (and *FUL*) and that AHLs act downstream of SOC1 (and FUL) as key regulators of AM maturation (Fig. 10).

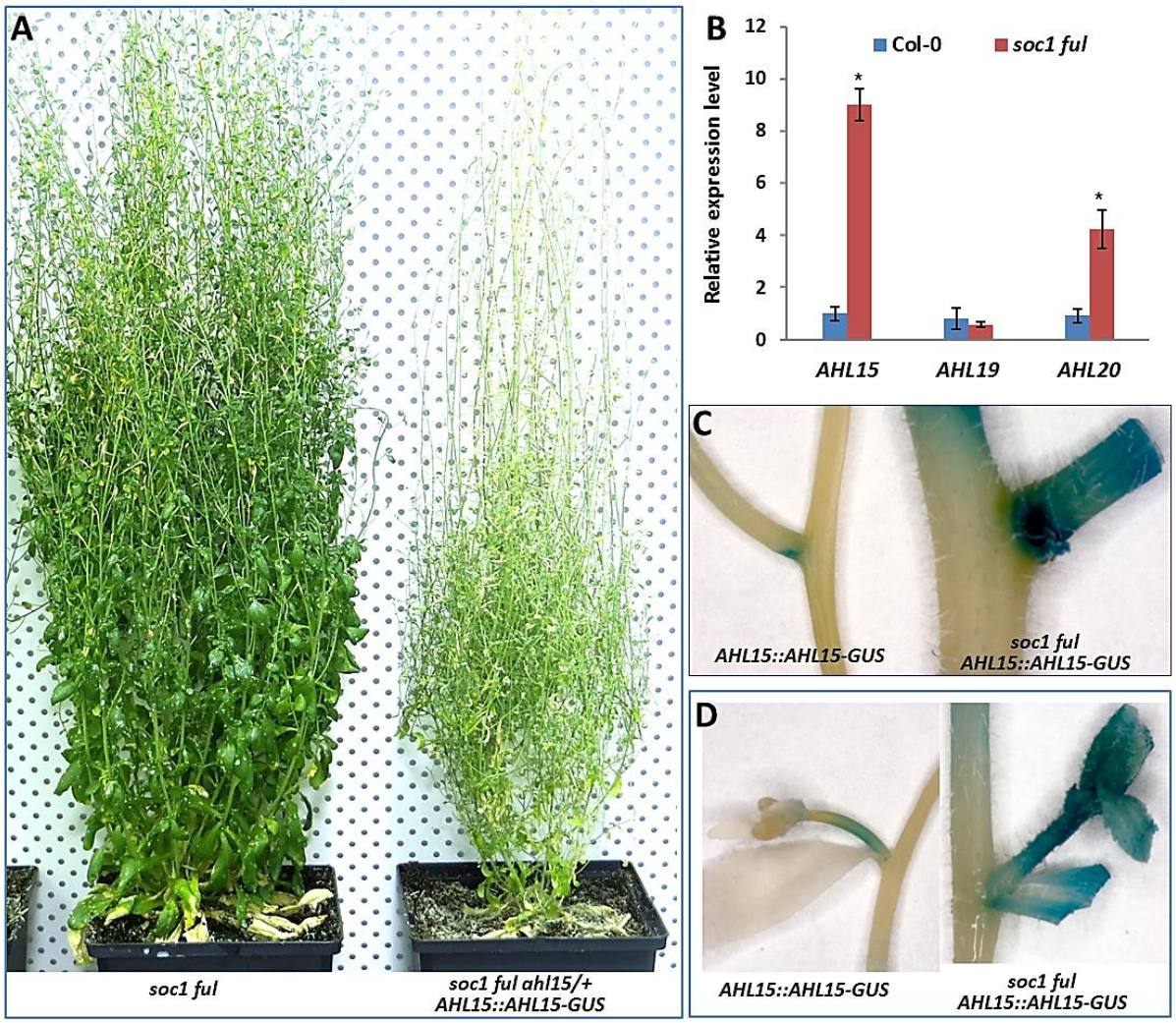

Figure 9 *AHL* genes are essential for the polycarpic behaviour of *Arabidopsis soc1 ful* mutant plants. (A) Comparison of a four-month-old *soc1 ful* mutant with many aerial rosettes (left) and a more wild-type looking *soc1 ful ahl15/+ AHL15::AHL15-GUS* plant (right) both grown in LD. (B) qPCR analysis of *AHL15*/*19*/*20* expression in inflorescence nodes of wild-type (Col-0) and *soc1 ful* plants 2 weeks after flowering. Asterisks indicate a significant difference in expression level in mutant compared to wild-type plants (Student's *t*-test, $p < 0.001$) and error bars indicate the standard error of the mean of three biological replicates. (C and D) GUS activity staining showing *AHL15::AHL15-GUS* expression in an inflorescence node (C) or a lateral inflorescence (D) of wild-type (left) and *soc1 ful* (right) plants at a comparable developmental stage.

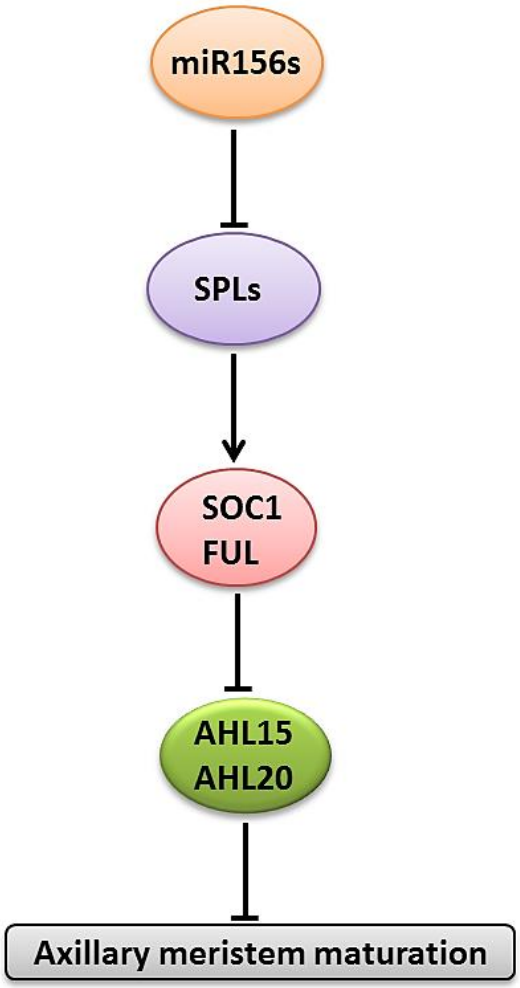

Figure 10 Proposed model for the key role for AHL genes in controlling AM maturation downstream of Ageing (SPL) and flowering (SOC1 and FUL) genes. It is well established that miR156 controls the action of SPL proteins in promoting the floral transition by directly activating the flowering genes *SOC1* and *FUL* (Wang et al., 2009a; Yamaguchi et al., 2009). Here we show that *AHL* genes, of which *AHL15/RJV* has been previously identified as direct downstream target of *SOC1* (Immink et al., 2012a; Tao et al., 2012), are repressed by the SPL-SOC1/FUL pathway, and that they are directly responsible for the delay in flowering and the vegetative growth from axillary meristems observed in the *spl* or *soc ful* loss-of-function or knock-down mutant lines. Enhanced *AHL* expression bypasses the SPL-SOC1/FUL pathway and turns monocarpic *Arabidopsis* into a polycarpic plant by maintaining some axillary meristems in a vegetative state. Arrows indicate gene activation, and blunted lines indicate repression.

Discussion

Flowering plants age through several well-defined developmental phase transitions, starting with the embryonic to juvenile phase change, and ending with the adult vegetative to generative transition, which in annual monocarpic plants preludes senescence and plant death (Amasino, 2009). Here we show that the *Arabidopsis* AT-hook protein *RJV/AHL15* and related paralogs act as master regulators of ageing, as their expression induces meristem rejuvenation, causing annual monocarpic plants such as *Arabidopsis* and tobacco to become

polycarpic, perennial plants. This newly discovered function of AHL proteins is conserved in at least three families of flowering plants (Brassicaceae, Solaneaceae and Fabaceae). Reversion of developmental phase transitions by overexpression of key regulators has been reported before (Lotan et al., 1998; Stone et al., 2001; Boutilier et al., 2002; Zuo et al., 2002), but this is the first time that reversion was observed for all developmental phase transitions. This suggests that AHL15/RJV and its family members play a central role in all these developmental phase transitions, and that regulation of their expression can delay plant development and change a plant's life history. In fact, *Arabidopsis* when grown under SD conditions can adopt polycarpic traits such as aerial rosette, and the enhanced *AHL15* expression in axillary meristems under SD conditions suggests that *AHL15/RJV* is involved in the plant's response to environmental triggers. Moreover, the existence of both mono- and polycarpic species within many plant genera indicates that life history traits changed frequently during evolution (Amasino, 2009). As *AHL* gene families have been identified in monocarpic and polycarpic plant species (Zhao et al., 2014), we hypothesize that *AHL* genes are key evolutionary targets for modulating monocarpic to polycarpic growth.

AHL proteins are DNA-binding proteins, and as in animals they are able to remodel chromatin (Lim et al., 2007; Ng et al., 2009). The mode of action of AHL proteins is largely unknown, and therefore one of the objectives of our future research will be to unravel the molecular mechanisms by which these proteins influence plant developmental phase transitions. One gene family encoding transcription factors involved predominately in plant tissue ageing are the *SPL* genes, which are known to orchestrate the adult developmental program, and are highly upregulated in adult leaves and during flowering (Wu and Poethig, 2006; Wu et al., 2009). The age-related function of *AHL* genes might potentially be mediated by repression of *SPL* gene expression.

Our findings create new possibilities for applications in crop breeding and in agri- and horticultural practices. Monocarpic crops require more fertilizer and herbicides than polycarpic plants, which can have negative effects on productivity and biodiversity(Asbjornsen et al., 2013; Armstrong et al., 2012). Converting monocarpic crop plants with a single harvest of seeds, flowers or fruits into polycarpic plants, permits multiple harvests without the need for sowing and replanting. Such plants do not have to invest resources into a new root system, and since their root system grows deeper, there will be less need for watering and a reduced chemical runoff and soil erosion (Armstrong et al., 2012). Moreover, longer photosynthetic activity and greater root mass in polycarpic plants increase plant productivity (Glover et al., 2010), which holds promise for future environment and food security (Werling et al., 2014). Based on our results, we expect that perennialized crops can be obtained by spatio-temporal enhancement of *AHL* gene expression through CRISPR/Cas9-based technology (Woo et al., 2015).

Methods

Plant material and growth conditions

All *Arabidopsis* mutant- and transgenic lines used in this study are in the Columbia (Col-0) background. The *ahl15* and *ahl19* T-DNA insertion mutants (SALK_040729C and

SALK_070123) and the previously described *spl9-4 spl15-1*, *soc1-6 ful-7*, *35S::miR165*, *35S::MIM156* and *SPL9::rSPL9* lines (Wang et al., 2009a) were obtained from the Nottingham *Arabidopsis* Stock Centre (NASC). The reporter lines *pSPL9::SPL9-GUS*, *pSPL9::rSPL9-GUS* (Yang et al., 2011) and *pmiR156A::GUS*, *pmiR156B::GUS*, and *pmiR156A::GUS* (Yu et al., 2015) have been described previously. Seeds were germinated after three days incubation at 4°C on MA medium (Masson and Paszkowski, 1992) containing 1% sucrose, and 0.7% agar at 21 °C under a 16 hour photoperiod, and seedlings were transferred to soil and grown at 21 °C under 65% relative humidity and long-day (LD: 16 hour photoperiod) or short-day (SD: 12 hours photoperiod) conditions. To score phenotypes such as maintenance of juvenility, rejuvenation, and longevity, Col-0 wild-type and overexpression plants were transferred to larger pots about 3 weeks after flowering and after harvesting ripened siliques. Vegetative phase changes and flowering time were determined under long-day (LD; 16 hours photoperiod and 70% relative humidity at 21°C) or short-day (SD; 12 hours photoperiod and 70% relative humidity at 21°C) conditions. *Nicotiana tabacum* (cv SR1 Petit Havana) plants were grown in medium-sized pots at 25 C° temperature, 75% relative humidity and 16 hours photoperiod. For dexamethasone (DEX, Sigma-Aldrich) treatment, *Arabidopsis* seeds were germinated on MA medium containing 20 µM DEX or soil grown plants were sprayed with 20 µM DEX. Tobacco seeds were germinated on ½ MS medium containing 10 µM DEX, and seedlings or plants were sprayed with 30 µM DEX.

Plasmid construction and plant transformation

The *35S::AHL15* construct was generated by PCR amplification of the full-length *AHL15* cDNA of (AT3G55560) from ecotype Columbia (Col-0) using primers 35S::AHL15-F and -R (Table S1), and the resulting PCR product was cloned as a *Sma*I/*Bgl*II fragment into the *p35S-3'OCS* expression cassette of plasmid pART7, which was subsequently cloned as *Not*I fragment into the binary vector pART27 (Gleave, 1992). To generate the other overexpression constructs, the full-length cDNA clones of *AHL20* (AT4G14465), *AHL27* (AT1G20900), *AHL29* (AT1G76500) from *Arabidopsis* Col-0, *AC129090* from *Medicago trunculata cv* Jemalong, and *Bo-Hook1* (AM057906) from *Brassica oleracea* var *alboglabra* were used to amplify the open reading frames (ORFs) using primers indicated in Table S1. The ORFs were cloned into plasmid pJET1/blunt (GeneJET™ PCR Cloning Kit, #K1221), and subsequently transferred as *Not*I fragments to binary vector pGPTV 35S-FLAG (Becker et al., 1992). To construct *35S::AHL15-GR*, a synthetic *Pst*I-*Xho*I fragment containing the *AHL15-GR* fusion was used to replace the BBM-GR fragment in binary vector pSRS031 (Passarinho et al., 2008). To generate the *AHL15::AHL15-GUS* and *pAHL15::AHL15-tagRFP* translational fusions, a 4 kb fragment containing the promoter and exon-intron sequences of *AHL15* was amplified using PCR primers AHL15-GUS-F and -R (Table S1), and inserted into pDONR207 via a BP reaction (Gateway, Invitrogen). LR reactions were carried out to fuse the 4 kb fragment upstream of GUS or tagRFP in destination vectors pMDC163 (Karimi et al., 2007) or pGD121 (Immink et al., 2012). All binary vectors were introduced into *Agrobacterium tumefaciens* strain AGL1 by electroporation (Den Dulk-Ras

and Hooykaas, 1995) and *Arabidopsis* Col-0 was transformed using the floral dip method (Clough and Bent, 1998).

Tobacco transformation

Round leaf discs were prepared from the lamina of 3rd and 4th leaves of 1-month-old soil grown tobacco plants. The leaf discs were surface sterilized by three washes with sterile water followed by incubation in 10 % glorix for 20 minutes (Baltes et al., 2014), and then again 4 to 5 washes with sterile water. The surface sterilized leaf discs were syringe infiltrated with an overnight acetosyringone (AS)-induced culture of *Agrobacterium tumefaciens* strain AGL1 containing binary vector pSRS031 (grown to OD_{600}= 0.6 in the presence of 100 µM AS) carrying the *35S::AHL15-GR* construct and co-cultivated for 3 days in the dark on co-cultivation medium (CCM). CCM consists of full strength MS medium (Murashige and Skoog, 1962) with 3% (w/v) sucrose (pH 5.8) solidified with 0.8 % (w/v) Diachin agar and supplemented with 2mg/l BAP, 0.2mg/l NAA and 40mg/l AS. After co-cultivation, the explants were transferred to CCM supplemented with 15mg/l phosphinothricin (ppt) for selection and 500mg/l cefotaxime to kill *Agrobacterium*. Regeneration was carried out at 24C° and 16 hours photoperiod. The regenerated transgenic shoots were rooted in big jars containing 100 ml hormone free MS medium with 15mg/l ppt and 500 mg/l cefotaxime. The rooted transgenic plants were transferred to soil and grown in a growth room at 25 °C, 75% relative humidity and a 16 h photoperiod. All the transgenic plants were checked for the presence of the T-DNA insert by PCR on genomic DNA extracted from leaf tissues using the CTAB method (Doyle, 1990).

Histolochemical staining, tissue fixation and microscopy

Histochemical β-glucuronidase (GUS) staining of transgenic lines expressing GUS was performed as described previously (Anandalakshmiet al.,1998). Tissues were stained for 4 hours at 37 °C, followed by rehydration by incubation for 10 minutes in a graded ethanol series (75, 50, and 25 %). GUS stained tissues were observed and photographed using a LEICA MZ12 microscope (Switzerland) equipped with a LEICA DC500 camera.

For scanning electron microscopy (SEM), fresh leaves were fixed in 0.1 M sodium cacodylate buffer (pH 7.2) containing 2.5% glutaraldehyde and 2% formaldehyde. After fixation, samples were dehydrated by a successive ethanol series (25, 50, 70, 95, and 100 %) and subsequently critical-point dried in liquid CO2. Dried specimens were gold-coated and examined using a JEOL SEM-6400 (Japan).

Quantitative real-time PCR (qPCR) analysis

RNA isolation was performed using a NucleoSpin® RNA Plant kit (MACHEREY-NAGEL). For qPCR analysis, 1 µg of total RNA was used for cDNA synthesis with the iScript™ cDNA Synthesis Kit (BioRad). PCR was performed using the SYBR-Green PCR Master mix (SYBR® Premix Ex Taq™, Takara) and a CFX96 thermal cycler (BioRad). The Pfaffl method was used to determine relative expression levels (Pfaffl, 2001). Expression was

normalized using *β-TUBULIN-6*. Three biological replicates were performed, with three technical replicates each. The primers used are described in Table S1.

Acknowledgements

We thank Kim Boutilier for critically reading the manuscript. This work is partially supported by Iranian Ministry of Science, Research, and Technology (MSRT 89100156)

References

Amasino, R. (2009). Floral induction and monocarpic versus polycarpic life histories. Genome Biol. **10**: 228.

Anandalakshmi, R., Pruss, G.J., Ge, X., Marathe, R., Mallory, A.C., Smith, T.H., and Vance, V.B. (1998). A viral suppressor of gene silencing in plants. Proc. Natl. Acad. Sci. **95**: 13079-13084.

Aravind, L. and Landsman, D. (1998). AT-hook motifs identified in a wide variety of DNA-binding proteins. Nucleic Acids Res. **26**: 4413–4421.

Armstrong, O.N., Glover, D., Reganold, J.P., and Cox, C.M. (2012). Plant perennials to save Africa ' s soils. Nature. **489**: 359–361.

Asbjornsen, H., Hernandez-Santana, V., Liebman, M., Bayala, J., Chen, J., Helmers, M., Ong, C.K., and Schulte, L. A. (2013). Targeting perennial vegetation in agricultural landscapes for enhancing ecosystem services. Renew. Agric. Food Syst. **29**: 101–125.

Baltes, N.J., Gil-Humanes, J., Cermak, T., Atkins, P.A, and Voytas, D.F. (2014). DNA replicons for plant genome engineering. Plant Cell **26**: 151–163.

Becker, D., Kemper, E., Schell, J., and Masterson. A. (1992). New plant binary vectors with selectable markers located proximal to the left T-DNA border. Plant Mol. Biol. **20**: 1195–1197.

Bleecker, B. and Patterson, S.E. (1997). Last exit: senescence, abscission, and meristem arrest in *Arabidopsis*. Plant Cell **9**: 1169–79.

Boutilier, K., Offringa, R., Sharma, V.K., Kieft, H., Ouellet, T., Zhang, L., Hattori, J., Liu, C., van Lammeren, A.A.M., Miki, B.L.A., Custers, J.B.M., and van Lookeren, M.M. (2002). Ectopic expression of *BABY BOOM* triggers a conversion from vegetative to embryonic growth. **14**: 1737–1749.

Clough, S.J. and Bent, F. (1998). Floral dip: a simplified method for *Agrobacterium*-mediated transformation of *Arabidopsis thaliana.* Plant J. **16**: 735–743.

Doyle, J.J. (1990). Isolation of plant DNA from fresh tissue. Focus (Madison). **12**: 13–15.

Den Dulk-Ras, A. and Hooykaas P.J.J (1995). Electroporation of *Agrobacterium tumefaciens*. Plant Cell Electroporation Electrofusion Protoc. **55**: 63–72.

Franco-Zorrilla, J.M., Valli, A., Todesco, M., Mateos, I., Puga, M.I., Rubio-Somoza, I., Leyva, A., Weigel, D., García, J.A., and Paz-Ares, J. (2007). Target mimicry provides a new mechanism for regulation of microRNA activity. Nat. Genet. **39**: 1033–1037.

Gerttula, S., Zinkgraf, M., Muday, G.K., Lewis, D.R., Ibatullin, F.M., Brumer, H., Hart, F., Mansfield, S.D., Filkov, V., and Groover, A. (2015). Transcriptional and hormonal regulation of gravitropism of woody stems in populus. Plant Cell **27**: 2800–2813.

Gleave, A.P. (1992). A versatile binary vector system with a T-DNA organisational structure conducive to efficient integration of cloned DNA into the plant genome. Plant Mol. Biol. **20**: 1203-1207.

Glover, J.D., Reganold, J.P., Bell, L.W., Borevitz, J., Brummer, E.C., Buckler. E.S., Cox, C.M., Cox, T.S., Crews, T.E., and Culman, S.W. (2010). Increased food and ecosystem security via perennial grains. Science. **328**: 1638–1639.

Hensel, L.L., Grbić, V., Baumgarten, D., and Bleecker, B. (1993). Developmental and age-related processes that influence the longevity and senescence of photosynthetic tissues in *Arabidopsis*. Plant Cell. **5**: 553–564.

Immink, R.G.H., Posé, D., Ferrario, S., Ott, F., Kaufmann, K., Valentim, F.L., de Folter, S., van der Wal, F., van Dijk, A.D.J., Schmid, M., and Angenent, G.C. (2012). Characterization of SOC1's central role in flowering by the identification of its upstream and downstream regulators. Plant

Physiol. **160**: 433–449.

Jarillo, J.A., Piñeiro, M., Cubas, P., and Martínez-zapater, J.M. (2009). Chromatin remodeling in plant development. **1596**: 1581–1596.

Karimi, M., Depicker, A., and Hilson, P. (2007). Recombinational cloning with plant gateway vectors. Plant Physiol. **145**: 1144–1154.

Kaufmann, K., Pajoro, A., and Angenent, G.C. (2010). Regulation of transcription in plants: mechanisms controlling developmental switches. Nat. Rev. Genet. **11**: 830–842.

Kishi, Y., Fujii, Y., Hirabayashi, Y., and Gotoh, Y. (2012). HMGA regulates the global chromatin state and neurogenic potential in neocortical precursor cells. Nat. Neurosci. **15**: 1127–1133.

Lim, P.O., Kim, Y., Breeze, E., Koo, J.C., Woo, H.R., Ryu, J.S., Park, D.H., Beynon, J., Tabrett, A., Buchanan-Wollaston, V., and Nam, H.G. (2007). Overexpression of a chromatin architecture-controlling AT-hook protein extends leaf longevity and increases the post-harvest storage life of plants. Plant J. **52**: 1140–1153.

Lotan, T., Ohto, M., Yee, K.M., West, M. a, Lo, R., Kwong, R.W., Yamagishi, K., Fischer, R.L., Goldberg, R.B., and Harada, J.J. (1998). *Arabidopsis LEAFY COTYLEDON1* is sufficient to induce embryo development in vegetative cells. Cell. **93**: 1195–1205.

Masson, J., and Paszkowski, J. (1992). The culture response of *Arabidopsis thaliana* protoplasts is determined by the growth conditions of donor plants. Plant J. **2**: 829-833.

Melzer, S., Lens, F., Gennen, J., Vanneste, S., Rohde, A., and Beeckman, T. (2008). Flowering-time genes modulate meristem determinacy and growth form in *Arabidopsis thaliana*. Nat. Genet. **40**: 1489–1492.

Munné-Bosch, S. (2008). Do perennials really senesce? Trends Plant Sci. **13**: 216–20.

Murashige, T., and Skoog., E.F. (1962) A revised medium for rapid growth and bio assays with tobacco tissue cultures. Physiol. Plant. **15:** 473–497.

Ng, K.-H., Yu, H., and Ito, T. (2009). AGAMOUS controls *GIANT KILLER*, a multifunctional chromatin modifier in reproductive organ patterning and differentiation. PLoS Biol. **7**: e1000251.

Passarinho, P., Ketelaar, T., Xing, M., van Arkel, J., Maliepaard, C., Hendriks, M.W., Joosen, R., Lammers, M., Herdies, L., den Boer, B., van der Geest, L., and Boutilier, K. (2008). BABY BOOM target genes provide diverse entry points into cell proliferation and cell growth pathways. Plant Mol. Biol. **68**: 225–237.

Pfaffl, M.W. (2001). A new mathematical model for relative quantification in real-time RT-PCR. Nucleic Acids Res. **29**: e45-e45.

Reeves, R. (2010). Nuclear functions of the HMG proteins. Biochim. Biophys. Acta. Gene Regul. Mech. **1799**: 3–14.

Stone, S.L., Kwong, L.W., Yee, K.M., Pelletier, J., Lepiniec, L., Fischer, R.L., Goldberg, R.B., and Harada, J.J. (2001). *LEAFY COTYLEDON2* encodes a B3 domain transcription factor that induces embryo development. Proc. Natl. Acad. Sci. **98**: 11806–11811.

Street, I.H., Shah, P.K., Smith, A.M., Avery, N., and Neff, M.M. (2008). The AT-hook-containing proteins SOB3/AHL29 and ESC/AHL27 are negative modulators of hypocotyl growth in *Arabidopsis*. Plant J. **54**: 1–14.

Tao, Z., Shen, L., Liu, C., Liu, L., Yan, Y., and Yu, H. (2012). Genome-wide identification of SOC1 and SVP targets during the floral transition in *Arabidopsis*. Plant J. **70**: 549–561.

Telfer, A., Bollman, K.M., and Poethig, R.S. (1997). Phase change and the regulation of trichome distribution in *Arabidopsis thaliana*. Development **124**: 645–654.

Usami, T., Horiguchi, G., Yano, S., and Tsukaya, H. (2009). The more and smaller cells mutants of

Arabidopsis thaliana identify novel roles for *SQUAMOSA PROMOTER BINDING PROTEIN-LIKE* genes in the control of heteroblasty. Development **136**: 955–964.

Wang, J.-W., Czech, B., and Weigel, D. (2009a). miR156-regulated SPL transcription factors define an endogenous flowering pathway in *Arabidopsis thaliana*. Cell **138**: 738–749.

Wang, R., Farrona, S., Vincent, C., Joecker, A., Schoof, H., Turck, F., Alonso-Blanco, C., Coupland, G., and Albani, M.C. (2009b). *PEP1* regulates perennial flowering in *Arabis alpina*. Nature **459**: 423–427.

Weigel, D.N.O. (1995). A developmental switch sufficient for flower initiation in diverse plants. Nature. **377**: 495–500.

Werling, B.P. et al. (2014). Perennial grasslands enhance biodiversity and multiple ecosystem services in bioenergy landscapes. Proc. Natl. Acad. Sci. U. S. A. **111**: 1652–7.

Woo, J.W., Kim, J., Kwon, S. Il, Corvalán, C., Cho, S.W., Kim, H., Kim, S.-G., Kim, S.-T., Choe, S., and Kim, J.-S. (2015). DNA-free genome editing in plants with preassembled CRISPR-Cas9 ribonucleoproteins. Nat. Biotechnol. **33**: 1162–1165.

Wu, G., Park, M.Y., Conway, S.R., Wang, J.-W., Weigel, D., and Poethig, R.S. (2009). The sequential action of miR156 and miR172 regulates developmental timing in *Arabidopsis*. Cell **138**: 750–759.

Wu, G. and Poethig, R.S. (2006). Temporal regulation of shoot development in *Arabidopsis* thaliana by miR156 and its target *SPL3*. Development **133**: 3539–3547.

Xiao, C., Chen, F., Yu, X., Lin, C., and Fu, Y.-F. (2009). Over-expression of an AT-hook gene, *AHL22*, delays flowering and inhibits the elongation of the hypocotyl in *Arabidopsis thaliana*. Plant Mol. Biol. **71**: 39–50.

Xu, Y., Wang, Y., Stroud, H., Gu, X., Sun, B., Gan, E.-S., Ng, K.-H., Jacobsen, S.E., He, Y., and Ito, T. (2013). A matrix protein silences transposons and repeats through interaction with retinoblastoma-associated proteins. Curr. Biol. **23**: 345–350.

Yamaguchi, A., Wu, M.-F., Yang, L., Wu, G., Poethig, R.S., and Wagner, D. (2009). The microRNA-regulated SBP-Box transcription factor *SPL3* is a direct upstream activator of *LEAFY*, *FRUITFULL*, and *APETALA1*. Dev. Cell **17**: 268–278.

Yang, L., Conway, S.R., and Poethig, R.S. (2011). Vegetative phase change is mediated by a leaf-derived signal that represses the transcription of miR156. Development **138**: 245–249.

Yu, N., Niu, Q.-W., Ng, K.-H., and Chua, N.-H. (2015). The role of miR156/SPLs modules in *Arabidopsis* lateral root development. Plant J. **83**: 673–85.

Yun, J., Kim, Y.-S., Jung, J.-H., Seo, P.J., and Park, C.-M. (2012). The AT-hook motif-containing protein AHL22 regulates flowering initiation by modifying *FLOWERING LOCUS T* chromatin in *Arabidopsis*. J. Biol. Chem. **287**: 15307–15316.

Zhao, J., Favero, D.S., Peng, H., and Neff, M.M. (2013). *Arabidopsis thaliana* AHL family modulates hypocotyl growth redundantly by interacting with each other via the PPC/DUF296 domain. Proc. Natl. Acad. Sci. **110**: E4688–E4697

Zhao, J., Favero, D.S., Qiu, J., Roalson, E.H., and Neff, M.M. (2014). Insights into the evolution and diversification of the *AT-hook Motif Nuclear Localized* gene family in land plants. BMC Plant Biol. **14**: 2-19.

Zhou, C.-M., Zhang, T.-Q., Wang, X., Yu, S., Lian, H., Tang, H., Feng, Z.-Y., Zozomova-Lihová, J., and Wang, J.-W. (2013a). Molecular basis of age-dependent vernalization in *Cardamine flexuosa*. Science **340**: 1097–1100.

Zhou, J., Wang, X., Lee, J.-Y., and Lee, J.-Y. (2013b). Cell-to-cell movement of two interacting AT-hook factors in *Arabidopsis* root vascular tissue patterning. Plant Cell **25**: 187–201.

Zuo, J., Niu, Q.-W., Frugis, G., and Chua, N.-H. (2002). The *WUSCHEL* gene promotes vegetative-to-embryonic transition in *Arabidopsis*. Plant J. **30**: 349–359.

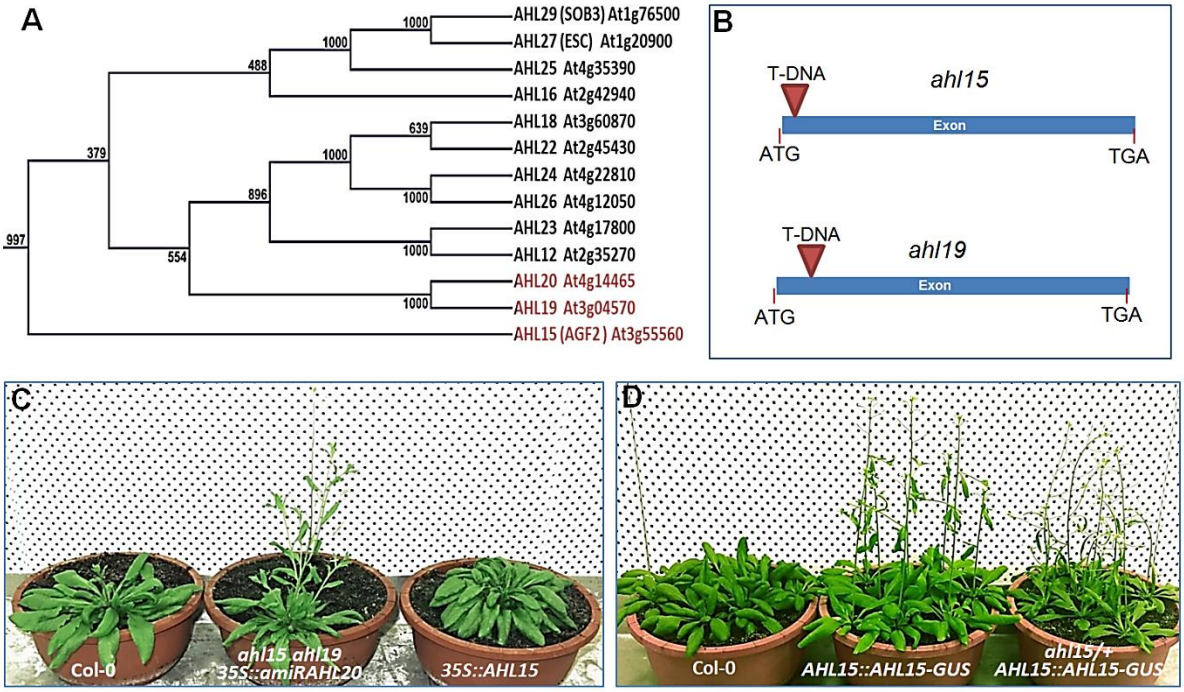

Supplementary figure 1 ***Arabidopsis AHL15*** **and close homologs redundantly regulate flowering time.** (A) Part of the phylogenetic tree of the *Arabidopsis* AHL protein family showing AHL15 and the closest paralogs. (B) Location of the T-DNA insertions in the *ahl15* and *ahl19* loss-of-function mutants. Note that the *AHL15* and *AHL19* genes are intronless. (C) Early flowering phenotype of an *ahl15 ahl19 35S::amiRAHL20* plant and delayed flowering phenotype of a *35S::AHL15* plant, both grown under short days (SD). (D) Early flowering phenotypes of *AHL15::AHL15-GUS* (observed in 25 independent lines) and *ahl15/+ AHL15::AHL15-GUS* (observed in three independent *AHL15::AHL15-GUS* lines crossed with *ahl15*) plants grown under long days (LD).

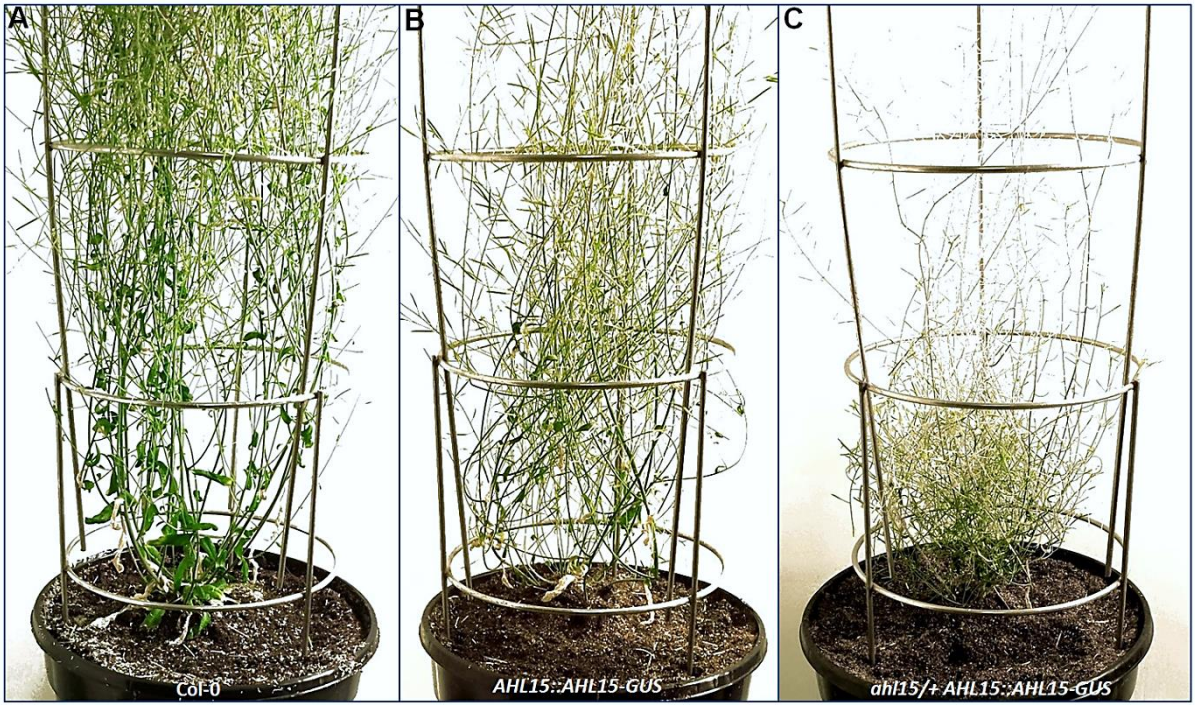

Supplementary figure 2 Early seed set and senescence of *Arabidopsis ahl* loss-of-function mutant plants. Two-month-old wild-type (Col-0) (A), *AHL15::AHL15-GUS* (B), or *ahl15/+ AHL15::AHL15-GUS* (c) *Arabidopsis* plants grown under LD.

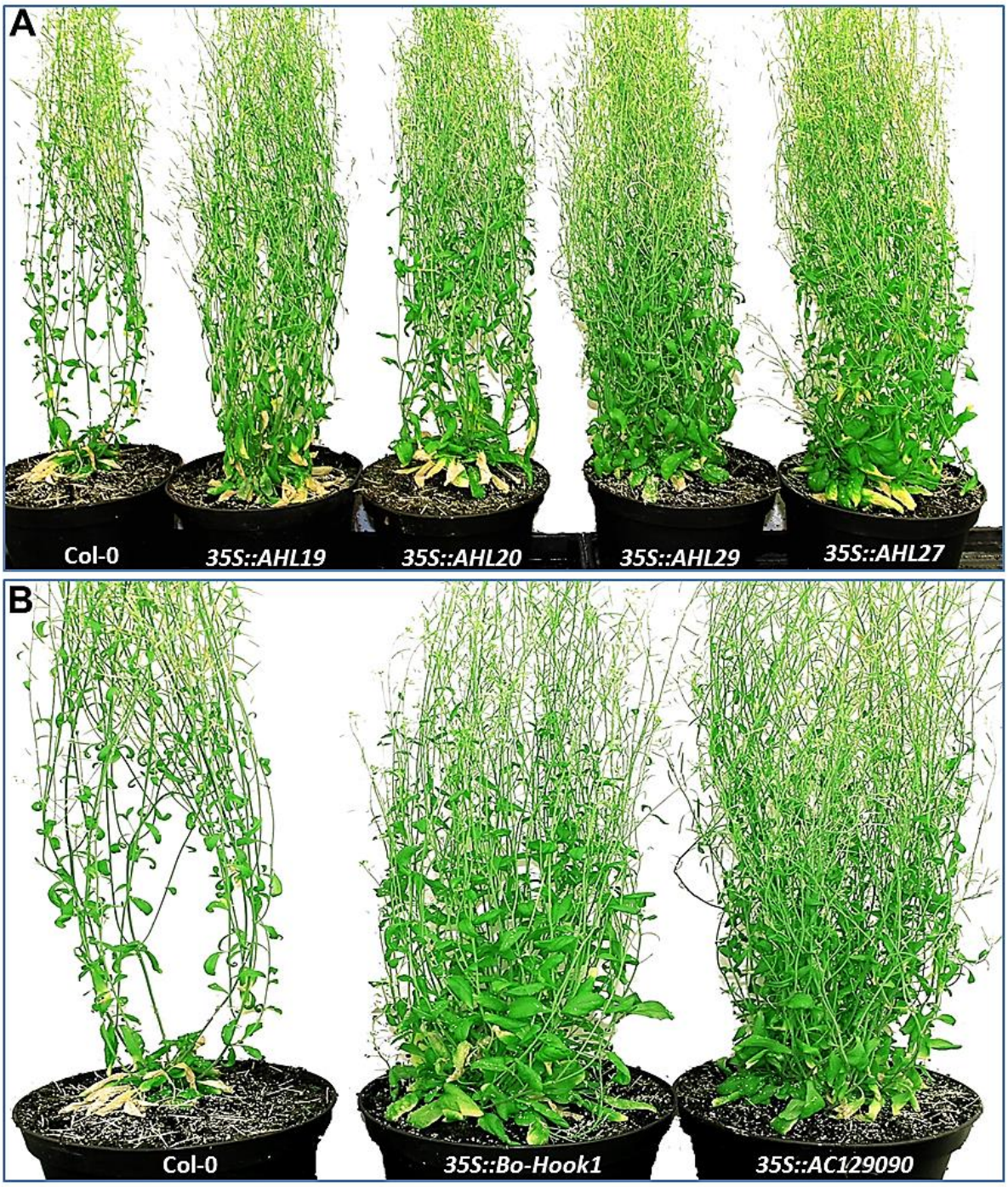

Supplementary figure 3 Overexpression of *Arabidopsis AHL15* paralogs or putative orthologs induces enhanced branching and aerial rosette formation in *Arabidopsis*. (A and B) Wild-type (Col-0) or transgenic *Arabidopsis* plants overexpressing *Arabidopsis AHL19*, *AHL20*, *AHL27* and *AHL29* (A), or the putative *AHL15* orthologs from *Brassica oleracea* (*Bo-Hook1*) or *Medicago trunculata* (*AC129090*) (B). Plants were grown under LD.

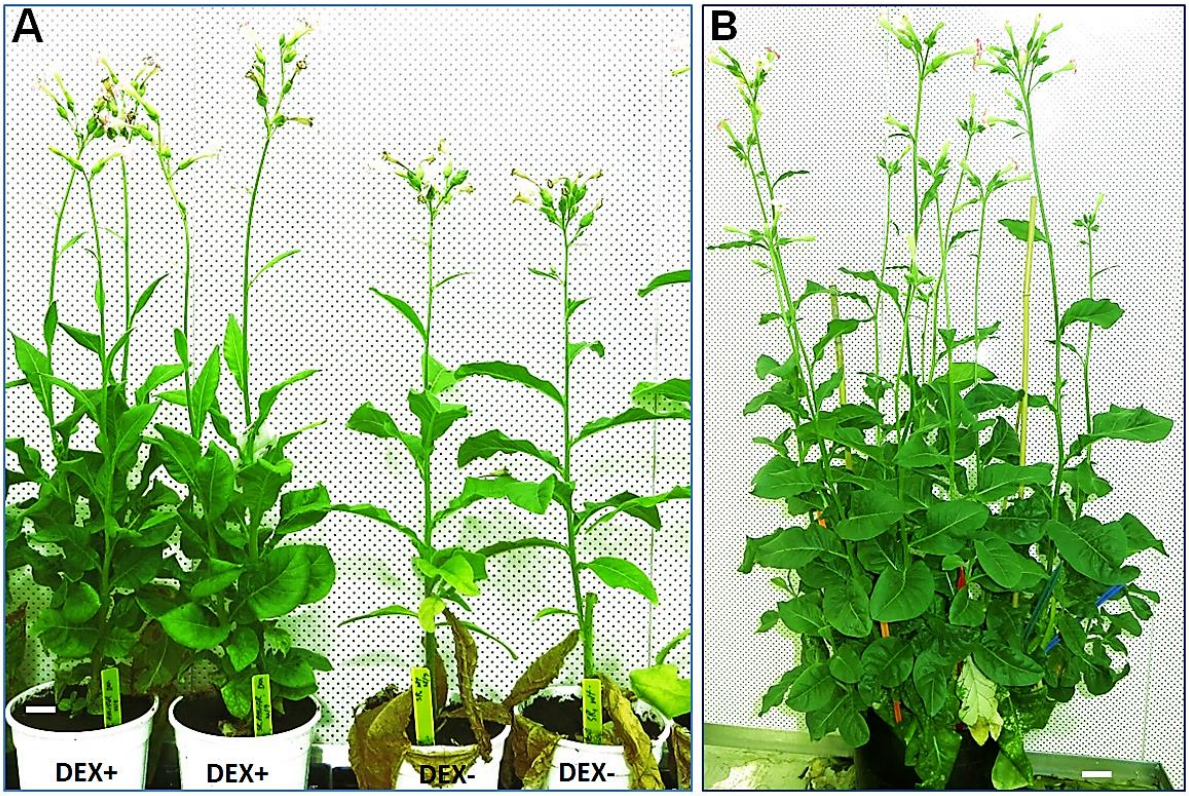

Supplementary figure 4 Induction of polycarpy and reduced senescence in tobacco plants overexpressing *Arabidopsis AHL15*. (A) Induction of axillary meristem activity in flowering *35S::AHL15-GR* tobacco plants sprayed with 30 μM DEX (left). Axillary meristem activity and delayed senescence was not observed in mock treated *35S::AHL15-GR* plants (right). (B) A two-year-old *35S::AHL15-GR* tobacco plant flowers treated with 30 μM DEX, after four previous cycles of DEX-induced rejuvenation and seed production. Size bars indicate 3cm in A and 5 cm in B.

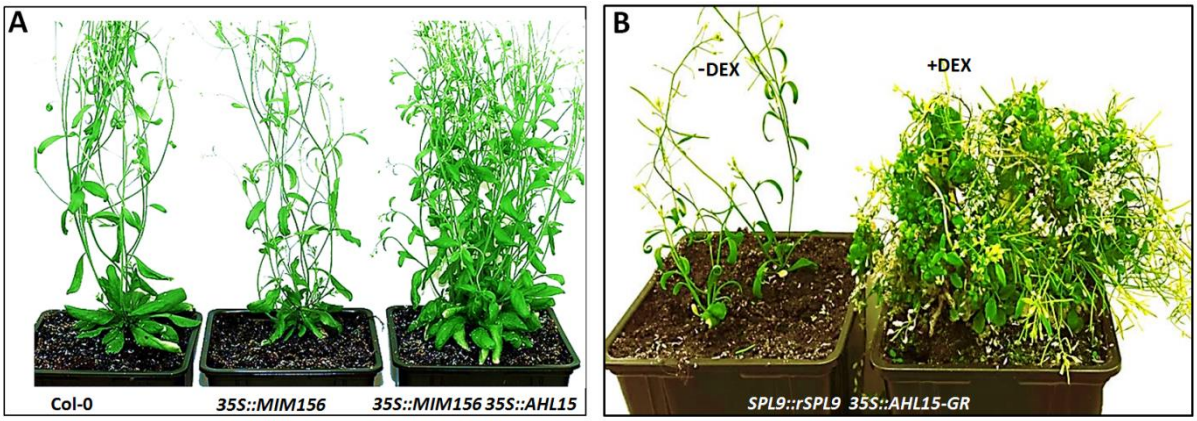

Supplementary figure 5 Ectopic expression of *AHL15* rescues precocious maturation of AMs caused by elevated SPL levels. (A) Mature shoot phenotype of a flowering wild-type plant (left) *35S::MIMR156* plant (middle) and a *35S::MIMR156 35S::AHL15* plant (right). (B) Mature shoot phenotypes of flowering of *35S::AHL15-GR* and *SPL9::rSPL9* double transgenic plants after mock sprayed (-DEX) (left) and sprayed with 20 μM DEX (+DEX) (light). Plants were grown under LD.

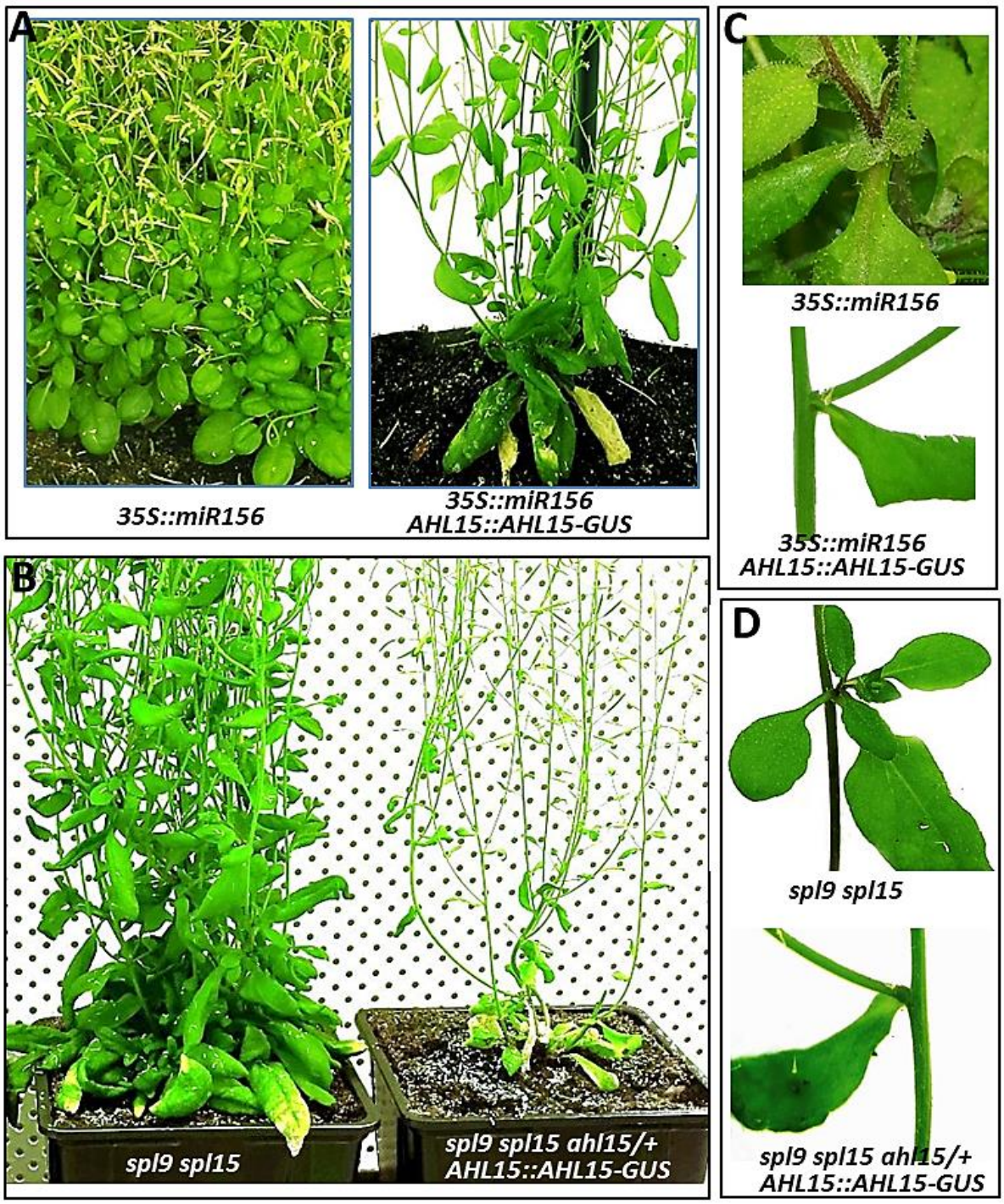

Supplementary figure 6 AHL function is essential for the suppression of AM maturation caused by reduced SPL levels. (A) Mature shoot phenotype of a flowering *35S::miR156* plant (left) and a *35S::miR156 AHL15::AHL15-GUS* plant (right). (B) Mature shoot phenotype of a flowering *spl9 spl15* plant (left) and a *spl9 spl15 ahl15/+ AHL15::AHL15-GUS* plant (right). (C) A lateral inflorescence with and without an aerial rosette on the first inflorescence node of a two-month-old *35S::miR156* (top) and *35S::miR156 AHL15::AHL15-GUS* plant (bottom), respectively. (D) A lateral inflorescence with and without an aerial rosette formed on the first inflorescence node of a two-month-old *spl9 spl15* (top) and *spl9 spl15 ahl15/+ AHL15::AHL15-GUS* plant (bottom), respectively. Plants were grown under LD. For presentation purposes, the original background of images in A (right panel), C and D was replaced by a homogeneous white background.

Supplementary figure 7 AHL function is essential for the polycarpic growth of *spl9 spl15* plants.
Phenotype of 5 month-old *spl9 spl15* (A) and *spl9 spl15 ahl15/+ AHL15::AHL15-GUS* (B) plants. Plants were grown under LD.

Supplementary Table 1: PCR primers used for cloning, genotyping, or qRT-PCR.

Name*	**Sequence (5' to 3')**	**Purpose**
35S::AHL15-F	CCCGGGATGGCGAATCCTTGGTGGGTAG	*35S::AHL15* construct
35S::AHL15-R	GGATCCTCAATACGAAGGAGGAGCACG	
35S::AHL29-F	ATAAGAATGCGGCCGCGACGGTGGTTACGATCAATC	*35S::AHL29* construct
35S::AHL29-R	ATAGTTTAGCGGCCGCCTAAAAGGCTGGTCTTGGTG	
35S::AHL20 –F	ATAAGAATGCGGCCGCGCAAACCCTTGGTGGACGAAC	*35S::AHL20* construct
35S::AHL20-R	ATAGTTTAGCGGCCGCTCAGTAAGGTGGTCTTGCGT	
35S::AHL27-F	ATAAGAATGCGGCCGCGAAGGCGGTTACGAGCAAGG	*35S::AHL27* construct
35S::AHL27-R	ATAGTTTAGCGGCCGCTTAAAAAGGTGGTCTTGAAG	
35S::Bo-Hook-1-F	ATAAGAATGCGGCCGCGCGAATCCTTGGTGGGTAGA	*35S::Bo-Hook-1* construct
35S::Bo-Hook-1-R	ATAGTTTAGCGGCCGCTCAATATGAAGGAGGACCAC	
35S::AC129090-F	ATAAGAATGCGGCCGCTCGAATCGATGGTGGAGTGG	*35S::AC129090* construct
35S::AC129090-R	ATAGTTTAGCGGCCGCTCAATATGGAGGTGGATGTG	
35S::AHL19-F	GGGGACAAGTTTGTACAAAAAAGCAGGCTCGATGGC GAATCCATGGTGGAC	*35S::AHL19* construct
35S::AHL19-R	GGGGACCACTTTGTACAAGAAAGCTGGGTAAACAAG TAGCAACTGACTGG	
AHL15-GUS-F	GGGGACAAGTTTGTACAAAAAAGCAGGCTCGACACT CCTCTGTGCCACATT	*AHL15::AHL15-GUS* construct
AHL15-GUS-R	GGGGACCACTTTGTACAAGAAAGCTGGGTAATACGA AGGAGGAGCACGAG	
SALK_040729-F	GTCGGAGAGCCATCAACACCA	*ahl15* genotyping
SALK_040729-R	CGACGACCCGTAGACCCGGATC	
SAIL_150_B05-F	TGGTTCCTCCACTGAGTCATC	*spl9-4* genotyping
SAIL_150_B05-R	GCTCATTATGACCAGCGAGTC	
SALK_074426-F	TGTTGGTGTCTGAAGTTGCTG	*spl15-1* genotyping
SALK_074426-R	TCCACCGAGTCTTCTTCACTC	
soc1-6 -F	AAAGGATGAGGTTTCAAGCG	*soc1-6* genotyping
soc1-6 -R	ATGTGATTCCACAAAAGGCC	
ful-7-F	GACCCGTTTTCTTCTCCCTC	*ful-7* genotyping
qAHL15-F	AAGAGCAGCCGCTTCAACTA	PCR *AHL15*
qAHL15-R	TGTTGAGCCATTTGATGACC	
qAHL20-F	CAAGGCAGGTTTGAAATCTTATCT	qPCR *AHL120*
qAHL20-R	TAGCGTTAGAGAAAGTAGCAGCAA	
qAHL19-F	CTCTAACGCGACTTACGAGAGATT	qPCR *AHL19*
qAHL19-R	ATATTATACACCGGAAGTCCTTGGT	
qβ-TUBULIN-6-F	TGGGAACTCTGCTCATATCT	qPCR *β-TUBULIN-6*
qβ-TUBULIN-6-R	GAAAGGAATGAG GTTCACTG	

*, F: forward; R: reverse